Parametric Investigation of Continuous Drive Friction Welding of Dissimilar Steel Bars (AISI 304H and AISI 4130)

A thesis submitted in fulfillment of the requirements for the award of MSc. In Manufacturing System Engineering

By:Kinfe Weldetnsae
Under the guidance of
Dr. Anil Kumar (Ass. prof.) and Mr. Lingerew E

Faculty of Mechanical Engineering
Jimma Institute of Technology
Jimma University

Jimma, Ethiopia
August,2020

DECLARATION

I hereby declare that this research paper entitled" Parametric Investigation of Continuous Drive Friction Welding of AISI (304H) and AISI (4130) Using a Lathe for an Application of Shafts" is my original work carried out with the supervision of Dr. Anil Kumar (Asst. prof.) and Mr. Lingerew E. No portion of the work referred to this thesis has been submitted in support of an application for any qualification of this or any other university or other institutes of learning.

Candidate:Kinfe Weldetnsae

Signature:_____ Date:_____

Advisor:Dr. Anil Kumar (Asst. prof.)

Signature:_____ Date:_____

Co-Advisor: Mr. Lingerew Enbakom

Signature:_____ Date:_____

Approved by:

Internal Examiner: Dr. Mesay Alemu

Signature:_____ Date:_____

External Examiner: Dr. Besufekad Negash

Signature:_____ Date:_____

ACKNOWLEDGEMENT

Praise to the omnipotent GOD who guided me all through my life to this very moment; and my great gratitude to my beloved wife who encourages me as a friend, a college, and a mentor; thank you love. Despite all the hard work I put in, this wouldn't be possible without the backup I got from my pals; Mohammed Indris and Samuel Tadesse who I hope to pay forward their favors. Besides, I want to address my sincere appreciation and thanks to my advisor Dr. Anil Kumar on his contribution to my study through his critical advice and comments. Last but not least, I want to address my utmost gratitude to Mr. Kidu.A and Dr. Eng Fred from Federal of Technical and Vocational Training Institute, Addis Ababa, Ethiopia, to Mr. Derege B; from Metals Industry Development Institute Addis Ababa, Ethiopia, and Mr. Temam M and all his colleges; from Burka Gibbe, Jimma, Ethiopia for their sincere and endeavored bolster to succeed in my study.

ABSTRACT

Friction welding is a solid-state joining process that merges materials under compressive force contact of workpieces rotating or moving relative to one another. Conventional fusion welding of dissimilar steel bars is not feasible due to various draw backs; hence friction welding is one of the least sensitive of all welding methods for joining materials with wide differences in physical properties, since the heat is generated directly at the weld where the bond is to be developed. The purpose of the current study is to investigate parameters(rotational speed, friction time, and burn-off length) continuous drive friction welding in joining both AISI 304H and AISI 4130 steel bars using universal lathe machine. Chemical composition of the materials is tested in a spectrometer. Response surface methodology is used for designing the experiment. Tensile strength and microhardness of the weldment is investigated to identify their mechanical properties. The tensile strength increased steadily as the rotational speed increased, it also increased up to some amount and started declining when the friction time gets higher, and it decreases when the burn of length was in its least and higher level. The hardness of the weldment is higher at the weld interfaces and showed an inverse relationship with the strength of weldment. Optimization is carried out by response surface methodology. Besides, the working temperature is measured using infrared thermometer and the tensile strength of the weldment exhibits an adequate joining of the dissimilar steel bars; thus maximum tensile strength is found in the weakest part of AISI 304H bar.

Keywords: *Continuous Drive Friction Welding, AISI 304H, AISI 4130, Friction time, Rotational speed, Burn-off length, Response surface methodology*

Contents

List of Figures

List of Tables

ACRONYMS

2D Two Dimensional

3D Three Dimensional

AC Alternative Current

AISI American Iron and Steel InstituteANOVA Analysis of Variance

ASTM American standard testing machine

BL Burn-Off Length

C Carbon

CDFW Continuous Drive Friction Welding

CI Confidence Interval

Cr Chromium

CS Carbon Steel

CTE Coefficient of Thermal Expansion

DC Direct Current

DF Degree of Freedom

DOE Design of Experiment

EBW Electron beam welding

FCC Face Centered Cubic

FT Friction Time

GTAW Gas Tungsten Arc Welding

HAZ Heat Affected Zone

HRC Rockwell hardness

HT Heat Treatment

ISO International Standard Organization

LBW Laser Beam Welding

Lc Grip to Grip Length

LT Total Length

Mn Manganese

Mo Molybdenum

P Phosphorus

S Sulfur

SAE Society of Automotive Engineers

SAW Submerged Arc Welding

Si v

SMAW Shield Metal Arc Welding

SS Stainless Steel

UTS Ultimate Tensile Strength

1 INTRODUCTION

1.1 Background

Continuous friction welding is one of the solid state welding methods, which is gaining higher importance among others. Latest developments in control systems and other technological facilities increase the applicability of the method for the welding of noncircular cross-sectioned components despite its convenience for components having circular cross-sections [1]. It is one of the most effective processes for joining similar and dissimilar materials with high joint integrity [2]. A few decades ago, materials were categorized as weldable and non-weldable, but innovations in technology enabled the joining of most of materials by fusion and solid state welding techniques. Typical fusion welding techniques include: gas welding (Oxyacetylene), arc welding (SMAW, GTAW, and SAW), high energy beam welding (EBW and LBW), plasma and laser welding. Heat sources for these techniques are a gas flame, an electric arc, and a high beam, respectively. However, in the nature of these techniques, rapid heating can cause damage to the work piece, including weakening and distortion [3]. Friction welding is one of the solid state welding processes and it is the least sensitive of all welding methods for joining materials with wide differences in physical properties, since the heat is generated directly at the weld where the bond is to be developed [4]. It is used widely in recent years due to its prominent gains and advantages on low production time, low heat input, and ease of manufacture and, the selection of welding conditions compared to other welding methods. Hence, it is most economical and high productive method for various applications of aerospace, automotive and chemical industries. The joining of ferrous and nonferrous materials either in similar or dissimilar combinations, which are not able to join by using fusion welding methods, can be successfully joined by friction welding method[5].

1.2 Friction Welding

It is a solid-state joining process that joins either similar or dissimilar components having different or the same chemical composition and produces high-quality welds between components[6]. Parts to be welded are brought in contact against each other to create heat at the interface of the welds which softens the materials on both sides of the friction faces. Once enough heat has generated the softened material tends to flow to either side to create coalesce and initiates a weld; meanwhile, the rubbing action is ceased and the contact pressure is maintained or increased for a while, to promote the solid-phase bond. Therefore, in this case, a machine that can change mechanical energy into heat

energy at the joint interface using relative movement between workpieces is required[7].

The definition of friction welding in the American Welding Society (AWS) C6.1-89 standard is as follows[8]:

'Friction welding is a solid-state joining process that produces coalescence of materials under compressive force contact of workpieces rotating or moving relative to one another to produce heat and plastically displace material from the faying surfaces.' Under normal conditions, the faying surfaces do not melt. Filler metal, flux, and a shielding gas are not required with this process.

1.2.1 ***Process Variant***

Rotary, linear and orbital are the most common friction welding type's as shown below in Figure 1.1

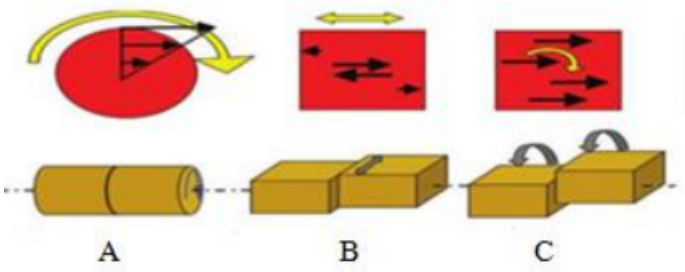

Fig. 1.1: Three common type of friction welding[9]

(A) Rotary friction welding: is the most frequently used method where one component is rotated around its axis while the other remains stationary. The two components are brought together under a certain friction pressure.

(B) Linear friction welding: the parts move under pressure relative to each other in a reciprocating fashion through a small linear displacement (amplitude) in the plane of the joint to be made.

(C) Orbital friction welding: makes the welding of irregularly shaped plastic parts possible. In linear vibration welding, the surfaces to be joined are rubbed together in an oscillating,linear motion under pressure applied at a 90^0 angle to the vibration.

As stated in [8, 28] rotary friction welding has the inherent limitation its inability to be used for non-circular cross-section components. Another main disadvantage is that the rate of heat generation is not uniform over the interface because of the linear variation of rotational speed with radial distance. This creates a non-uniform thickness of the heat-affected zone (HAZ) across the interface. Depending on how rotational energy is converted into frictional heat, rotary friction welding is divided into two major process variations:

1. **Continuous drive (direct energy) friction welding**: requires a constant energy source for any desired duration.

2. **Inertia drive (stored energy) friction welding**: uses the kinetic energy stored in a rotating flywheel.

1.2.2 *Continuous Drive Friction Welding (CDFW)*

In continuous drive friction welding, one of the parts is attached to a motor-driven unit while the other is restricted to stay still. When the motor-driven part rotates at a predetermined constant speed, the other part is being forced in to contact thereby Heat is generated; this continues for a predetermined time. Meanwhile, the motor brake turned off; afterward, the friction force is preserved or increased for a predetermined time after the rotation is ceased [27].

Process Stages

(A) Rotating part brought in to desired speed

(B) Friction phase; rotating part approaches and creates friction

(C) Heating phase; pressure is applied and rotation is maintained

(D) Forging phase; rotation stopped, pressure either maintained or increased as shown in Figure 1.2

Fig. 1.2: Process stages of direct drive friction welding[10]

Process Merits

The following listed advantages reasons make friction welding a reasonable welding type over fusion welding types [11],and [12]

- Creates narrow HAZ.
- not compatible for welding by other joining methods.
- The consistent and repetitive process of complete metal fusion.
- Joint preparation is a minimal saw-cut surface used most commonly.
- Faster Turn-around Times compared to the long lead time of forgings, which are currently 6 months or longer.
- Greatly increases design flexibility chooses appropriate material for each area of a blank. Suitable for diverse quantities from single prototypes to high-volume production.
- No fluxes, filler material, or gases required.
- Environmentally friendly process no fumes, gases, or smoke generated.
- Dissimilar metals are joined, even some considered incompatible or unweldable.

- The process is at least twice and up to 100 times as fast as other welding techniques.
- Friction welders are versatile enough to join a wide range of part shapes, materials, and sizes.
- Joint preparation isn't critically machined, saw cut, and even sheared surfaces are weldable.
- Resulting joints are of forged quality, with a 100% butt joint weld through the contact area.
- The machine-controlled process eliminates human error, and weld quality is independent of operator skill.
- It's ecologically clean with no objectionable smoke, fumes, or gases are generated that need to be exhausted.
- No consumables are required; no flux, filler material, or shielding gases.
- Power requirements are as low as 20% of that required of conventional welding processes.
- Since there is no melting, no solidification defects occur, e.g. gas porosity, segregation or slag inclusions

Fig. 1.3: Possible weldment combination of materials[13], and [14]

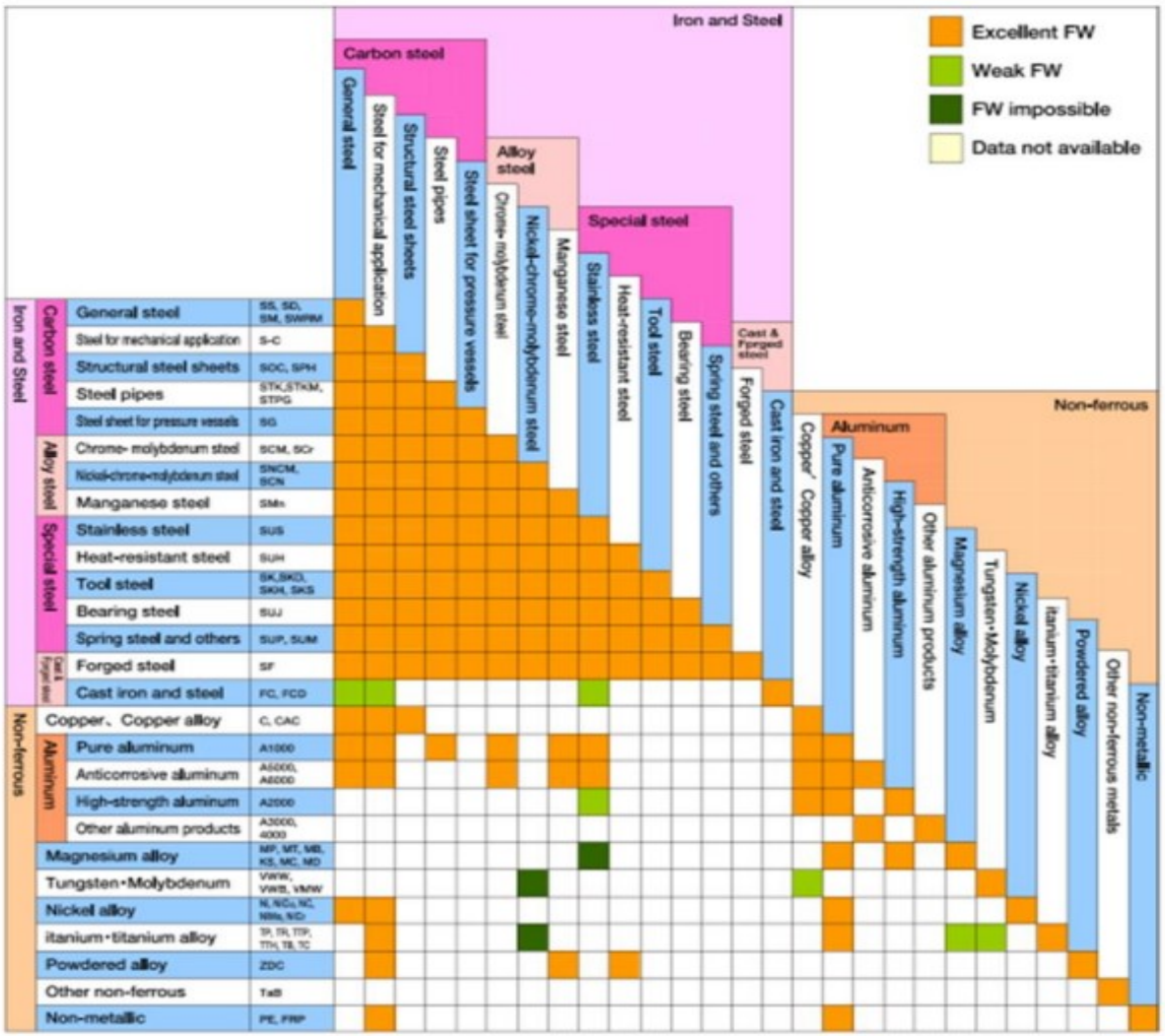

Process Applications

The applications of friction welding can be found in a wide range of industries from agriculture, automotive and aerospace to petroleum and electrical industries [15]; such as the manufacturing of valves, drive shafts and gear levers, applications in space parts industry such as radial-pump pistons and drill bits, and other applications in which the of materials is required [16]; see Table 1.1

Tab. 1.1: List of application areas of CDFW

No	Description	Material	Area of application
1	Wrought extension butterfly valves	SS-SS	Oil-Field Pieces
2	Front-axle yoke shaft	SAE1040	Agriculture and tracking
3	Torque rod to various bar stock	CS- SS	Agriculture and tracking
4	Marine outboard engine, drive shaft	CS- SS	Bimetallic and their special application
5	and Pump motor shaft	CS- SS	Bimetallic and their special application

Process Parameters

[1,17,29,30] divided the process in two phases;
(A) the friction phase, when the workpieces make contact, rubbing takes place between the friction surfaces and strong adhesion takes place at various contact points; and (B) the forging phase, during the end of the heating process when forging pressure is applied to the workpieces causing axial shortening. See Figure 1.4

Fig. 1.4: Process parameters of CDFW

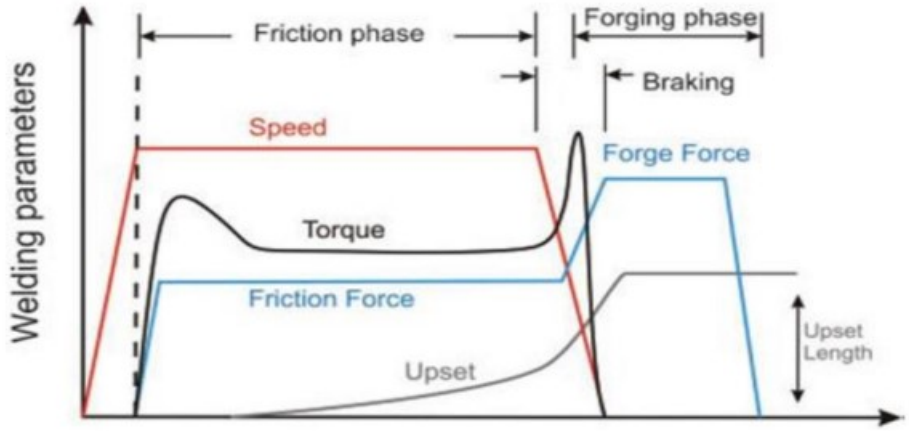

(A) Friction Phases: this phase can be subdivided into four stages [29], in the first stage, when the two pieces brought in to contact; sliding takes place between non-lubricated surfaces due to large axial force and inherent roughness on the two surfaces and creates an interlocking of aspirates. Strong adhesion joints and seizure are created at the points of real contact, shearing takes place at all junction when the material is weaker [17], thus the transfer of metal takes place from one surface to another. If one material is harder than the other, the harder material squeezes the softer material [18]. The size of the burn-off length and the rate of heat transfer depends on the temperature of the interface, the rubbing speed, and axial force [1, 30]. The second stage is a transition stage during which the layers of transferred fragments at the rubbing

interface become a layer of plasticized material offering less resistance. In the third stage, the rate of axial shortening and the equilibrium torque remains constant during this period. A plasticized layer is formed from the layer of originally transferred material. Thereby, in the last stage, deceleration and stopping took place and deep plasticized region moves outward thereby increases the thickness of the region. The torque decreases rapidly and similar low rubbing behavior is encountered as the first stage. The torque peak completes the plateau before it falls to zero very rapidly; thus the rate of axial shortening increases due to the increased amounts of material being pushed out into the collar.

(B) Forge stage: during this phase, the axial force is increased substantially to forge weld the two surfaces; and it helps in hot working the joint thereby increase the strength of the welds zone. Many studies [3],[5], and [12] reported that diffusion boned which has higher pressure higher than required has an imminent influence on the weld quality. Too high pressure result in large collars with metal being unnecessary extruded out. The HAZ can be reduced by pushing out the HAZ into the collar. Whereas low pressure does not expel impurities an there is no proper consolidation.

1.3 ***Stainless Steels and their Application***

Stainless steels are low-carbon steels with the addition of 4 to 6% chromium acquires good resistance to many of the corrosive media encountered in the chemical industry. This behavior is attributed to the formation of a strongly adherent iron chromium oxide on the surface. If more improved corrosion resistance and outstanding appearance are required, materials should be specified that use a superior oxide that forms when the amount of chromium in solution (excluding chromium carbides and other forms where the chromium is no longer available to react with oxygen) exceeds 12% [19]. When damaged, this tough, adherent, transparent, corrosion-resistant oxide (which is only 1 to 2 nm thick) heals itself, provided oxygen is present, even in very small amounts [20]. According to [21] Stainless steels can be divided into the following categories; austenite, ferrite, duplex martensite, and precipitation hardening

1.3.1 ***Austenitic Stainless Steels***

Austenitic stainless steels are easily identified by their nonmagnetic characteristic [4]. They are highly resistant to corrosion in almost all media (except hydrochloric acid and another halide acids and salts) and may be polished to a mirror finish, thereby combining the attractive appearance and corrosion resistance (See page 7,Table 1.2 for details).[16] Formability is outstanding (due to the low yield strength and high elongation that is characteristic of the FCC crystal structure), and these steels strengthen significantly when cold worked

Tab. 1.2: Types of austenite stainless steels and their description[8]

Grade	Description
301,301L,301LN	High strength for roll formed structural components
302HQ	Low work hardening rate grade for cold heading fasteners
303, 303Se	Free-machining bar grades
304, 304L, 304H	Standard 18/8 grades
310, 310S, 310H	High temperature resistant grades
316, 316L, 316H	Improved resistance to pitting corrosion in chloride environments
321, 321H, 347	Stabilized grades for heavy section welding and high temperature applications
253MA (S30815)	High temperature resistant grade
904L	High resistance to general corrosion, pitting and stress corrosion cracking

1.3.2 ***AISI 304H stainless steel***

This type of austenitic stainless steel offers the best combination of corrosion resistance and toughness of the stainless variety, is easily welded, and does not embrittle at low temperatures; and it is also the most costly stainless steel [16]. See page 8,Table 1.4(below).

Tab. 1.3: Mechanical and physical properties of AISI 304H stainless steel[8]

Mechanical properties	Tensile strength (MPa)		515
	Yield strength (MPa)		205
	Elongation (% in 50 mm)		40
	Rockwell hardness (HR C)		19
Physical properties	Density($\frac{kg}{m^3}$)		7900
	Elastic Modulus (GPa)		123
	Mean Coefficient of Thermal Expansion in($\mu/m/^0C$)	0-100^0c	17.2
		0-135^0c	17.8
		0-538^0c	18.4
	Thermal Conductivity ($\frac{W}{m.K}$)	0-100^0c	16.3
		500^0c	21.3
	Specific Heat(J/kg.K)	0-100°C	500

1.4 ***Low Alloy Steels***

Low alloy steels are iron-carbon alloys that contain additional alloying elements in amounts totaling less than about 5% by weight. Owing to these additions, low alloy steels have mechanical properties that are superior to those of the plain carbon steels for given applications. Superior properties usually mean higher strength, hardness, hot hardness; wear resistance, toughness, and more desirable combinations of these properties. Heat treatment is often required to achieve these improved properties. [8]Low alloy steels are not easily welded, especially at medium and high carbon levels. Since the 1960s, research has been directed at developing low carbon, low alloy steels that have better strength-to-weight ratios than plain carbon steels; but are less weldable than plain carbon steel steels.

1.4.1 ***AISI 4130 Steel***

This type of steel is one sort of low alloy steel which constitutes 30% of carbon Table 1-4 (below) illustrates; chemical, physical, and mechanical properties of the low alloy steel.

Tab. 1.4: Mechanical and physical properties of AISI 304H stainless steel[8]

Mechanical properties	Tensile strength (MPa)		890
	Treatment		HT
	Elongation (% in 50 mm)		17
	Rockwell hardness (HR C)		17
Physical properties	Density($\frac{kg}{m^3}$)		7700-8300
	Elastic Modulus (GPa)		190-200
	Mean Coefficient of Thermal Expansion in($\mu/m/^0C$)	0-100^0c	17.2
		0-135^0c	17.8
		0-538^0c	18.4
	Thermal Conductivity ($\frac{W}{m.K}$)	0-100^0c	16.2
		500^0c	21.5
	Specific Heat(J/kg.K)	0-100°C	500
	Electrical Resistivity ($n\Omega.m$)		720

HT implies heat treatment involving heating and quenching, followed by tempering to produce tempered martensite.

1.5 ***Motivations***

Conventional fusion welding of many dissimilar steel combinations is not feasible, because it leads to the formation of brittle and low melting inter-metallic phases due to metallurgical incompatibility, wide deference in melting point, and thermal mismatch [12]. Thus, welding dissimilar steel bars by fusion welding also create hot cracks due to inadvertent use of incorrect welding electrodes[10] which results in the formation of very hard, crack-susceptible bulk structure on the stainless steel side of the dissimilar metals. Least degree of segregation of the major alloying elements and minimization of the level of intermetallic phase in the weld metals as the result this makes the weldment of dissimilar metals difficult[11]. Owing to the merits of rotary friction welding as compared to conventional fusion welding technique; the continuous drive friction welding is of highly metals saving, low producing time, high quality, high efficiency and high-reliability characteristics[3]. And it is perhaps one of the least sensitive of all welding methods for joining materials with wide differences in physical properties, since the heat is generated directly at the weld where the bond is to be developed. Although most of the researchers of the related issues of the current study have studied welding of dissimilar steel bars of CDFW on a friction welder machine; very few studied using different lathe machines. The current study; parametric investigation of CDFW of AISI 304H and AISI 4130 using a lathe machine for an application of shafts has never been studied by any researcher so far. Thus, the current study deals with; experimental and statistical analysis of the CDFW samples to investigate the weld quality through tensile and micro-hardness assessment of the weldment.

1.5.1 ***Research Questions***

After the current study has put in to end, the following basic question of the research would have been addressed.

- How do the independent variables interact with each other in affecting the welding quality of the weldment?
- How do the independent variables interact independently in affecting the weld quality?
- What were the combination independent variables to happen a weaker weld quality?
- What were the combination independent variables to happen a strong weld quality?
- What does the recorded working temperature of each experiment imply?
- How does the microhardness variation in the HAZ affect the weld quality?
- What does the microhardness variation of the weld interface imply?
- Which combination of independent variation exhibit higher or lower hardness variation and why?
- What amounts of error were encountered in the examination and what were the reasons?
- What is the optimum optimized result gained from the design expert.
- What sort of model is fit for the experimental results? And what was the model significant?
- Is the lack of fit significant or non- significant?

1.6 ***Objectives***

1.6.1 ***General Objective***

The current studies general objective is to investigate continuous drive friction welding parameters of welded dissimilar steel bars which are: stainless steel (304H)) and low alloy steel (4130) materials in an arrangement of CDFW set up lathe machine.

1.6.2 ***Specific Objectives***

- To identify the working temperature of the experimentally welded samples using an infrared thermocouple
- To identify the chemical composition of the dissimilar steel bars using a spectrometer
- To create a CDFW set up in a lathe machine
- To carry out experiments using three independent variables (friction time, rotational speed, and burn of length)
- To carry out lab tests: tensile, microstructure, and hardness

- Infrared thermometer; temperature measuring apparatus
- To optimize the results obtained during lab tests using response surface methodology

1.7 ***Scope of the Study***

This study, parametric investigation of rotary friction welding of dissimilar steel bars, emphasizes in investigating only three independent parameters and three levels to identify their effects on the strength and hardness of the friction welded parts.

1.8 ***Limitation***

As mentioned in the foregoing, this study comprises only three parameters: friction time, rotational speed, and burn-off length. Other parameters which are included in rotary friction welding machines are excluded in this study because these were studied in detail by other researchers. In addition to that, the temperature rate of the experiment is not identified in the current study.

1.9 ***Delamination of the Study***

The current study is delaminated into five parts; the first part dealt with introduction, the second part dealt with methodology, the third part dealt with results and discussion, and the fourth part dealt with the conclusion and recommendation.

(I) Is all about introducing friction welding and explained thoroughly about its application, advantages and disadvantages, process parameters, stainless steels and low alloy steels,objectives, scope and limitations, motivation and research questions, and literature review.

(II) Illustrates the literatures of the related study of the current research

(III) Is all about the methodology of the study. In the methodology the first issue dealt with is selection of materials and apparatus and a research design. Following the research: Chemical composition test, experimental setup, experimental execution, laboratory tests (microstructural examination, microhardness test and tensile test) was carried out. Results from lab were thoroughly collected and thoroughly discussed using graphs and the possible reasons were explained compared to prior studies.

(V) A very precise conclusion are drawn and possible recommendation are pinpointed. Finally, future work of the study is also mentioned.

1.10 ***Significance of the Study***

The current study, as it is the first research of its kind, joining of AISI 4130 steel which is one of low alloy steel has joined with AISI 304H which is an austenite stainless steel has the following significance to the sponsored university and all sectors which are implementing a conventional joining methods

if they adopt the current study of welding method as a replacement or alternative specifically for round bars and hallow bars as well.

1.10.1 ***For Small Enterprises***

- It encourages small enterprises to utilize their lathe machines in hand without seeking a rotary friction welding machine.
- Owing to the merits of friction welding machines; the welding type avoids defective welded parts thus minimizes their profits.
- It minimizes the amount of hazards and reduces materials used during welding such as; welding electrodes and safety tools.
- It reduces production time and can be used for mass production by setting the machine only at the start.
- As the study has utilized design expert software for optimization purpose and encourages manufacturing industries to use this software for similar purpose.

1.10.2 ***For the Sponsored University***

- It enhances the area of research for dissimilar steel bars by one step ahead.
- As it is a pilot research of joining AISI 304H and AISI 4130, thus it will be useful for referencing purpose.
- It also encourages students to use design expert software as an optimization tool.

2

LITERATURE REVIEW

Up to this very moment, a lot of researchers have been working on rotary friction welding which is CDFW. Most of the researchers dealt with friction welding of materials which constitutes similar chemical composition and dimensions. Though very few researchers studied materials which comprise different chemical composition. Thus, almost all the researchers used a rotary friction welding machine to carry out their experiment except few researchers performed an experiment in a lathe machine by constructing a continuous drive set up, The related studies by different researchers are illustrated as follows;

[1]conducted a study which investigates the effect of a dimensional difference in friction welding of AISI 1040 specimen. In his study, he constructed a CDFW set up in a lathe machine to perform an experiment on a material which constitutes the same chemical composition. Prior to the final experiment, a pilot welding experiment was conducted in order to obtain optimum parameters according to the statistical approach. In this study, the strength of the friction welded specimen was predicted by the tensile testing machine to compare with the inherent strength of the material. In addition to that, the microstructure and hardness of the welded specimens were investigated.In this study, an optimum parameter was obtained by the optimization process, which is a simple linear model and the optimization process was carried out in a factorial design of experiments (DOEs) starting values were selected from the related issues of the same material. While optimization only two factors: friction pressure and friction time were optimized and while statistical analysis carried out involved two steps: confirming the adequacy of the model and finding the optimal estimated significant factors of the regression coefficients or least squares. During the optimization process, an optimal strength specimen was identified which constitutes the error in the least square method. Thus, the optimum parameters were found to be in the combination of 3s friction time and 30 MPa friction pressure by holding the upset time and upset pressure; 20s and 110 MPa respectively. Though the previously obtained optimum strength results were stage one and were carried on the same diametrical dimension of specimen. In the second stage, using the predefined optimum parameters, parts which comprise different dimensions were welded to identify the dimensional difference of the parts.

As a result of this study, it has been discussed as such that, welding parts that have a diametrical ratio of 3 tend to have the quality of 75% of the same diameter joints and the diametrical ratio of 4 tend to have 45% percent of the same diameter parts as well. In addition to that, parts with a width of 5mm contain 49% strength of the same materials.

In conclusion, it was manifested that the strength of the welded parts tends to decrease with an increase of dimensional difference of the welded parts and it was 3 diametrical ratios highly resembles an optimum strength of the diameter parts. Thus, the researcher arguably asserts that, having the predicted optimum parameters which are friction time and friction pressure; 3s and 30 MPa, and defining a definite friction time while increasing friction time and vice versa enhances the strength of the parts due to increased heat during the welding period. Thus; the researcher might be right in defining a definite pressure and increasing the friction time increases a heat during welding period thus increases the welding strength, but increasing the pressure and defining a definite friction time might not enhance the strength cause it tends to increase the burn-off length and decreases the strength of the welded material because it is highly likely that the source of heat is the rotational speed in friction welding.

In addition to the investigation, [2]the researcher studied the micro-hardness of the HAZ in order to relate the variation of the HAZ both vertically and horizontally starting from the interface of the welded parts and it has been understood that the hardness of the inherent material prior to the welding tends to increase in the heat-affected zone. Thus it was observed that the higher the diametrical difference the lower the strength of the welded parts. In this study Rotational speed was kept constant that the heat input was constant throughout the welded parts though the variation of hardness due to the heat loss when the dimensional difference of the parts gradually.

The researcher was also studied the microstructure of the heat-affected zone and inquires the effect of the microstructures in the strength of the welded parts. Thus it was observed that welded parts which constitute the same diameter tend to have both pearlite and ferrite structure and parts which comprises different diametrical ratio tend to constitute pearlite and ferrite structure with adjacent martensite structure. But when the diametrical ratio increases martensite structure tends to dominate the heat-affected zone. Thus, it decreases the strength.

In their study; Mechanical and microstructural properties of friction welded and effect of friction time on microstructure and mechanical properties of AISI 304 stainless steel to AISI 1060 steel[3] and [4] carried out an experiment in CDFW machine of 300 KN capacity at a constant rotation speed, and constant friction pressure (P1) and constant upsetting pressure (P2).

The friction time (t) was selected as three, five, and seven seconds. Tensile test specimens were prepared according to ASTM E8M-00b. Ultimate Tensile Strength (UTS) and yield strength of the welded specimens were determined. Hardness values (VH1) were determined. Prior to the experiment chemical composition was detected and welding parts were faced in to smooth surfaces and cleaned by a stainless steel brush and acetone to remove the oxides. The maximum hardness values of joints were obtained on the welding center line. The hardness values generally increased with friction time. Heat input, extensive plastic deformation, and degree of strain hardening were the cause for enhanced hardness in the welding interface which was related to the microstructure formed in the joint surface. Owing to the microstructural evaluations around the interface, diffusion of elements on the sides, work hardening, dislocation density, grain refinement, and formation of precipitations may cause this increase. Although the work hardening is effective on the SS side, phase transformation, fine grains, and formation of precipitates and rapid cooling from the welding temperature resulted in the hardening in the AISI 1060 steel. Due to cooling austenite transformation to the martensite formation was created and both sides of the materials were

hardened. It was observed that hardness values increased from the center through the thickness of the specimen.

The UTS strength corresponds to about 130% of that for the AISI 304 SS part and 81% of that for the AISI 1060 structural steel part. Although the UTS values were not influenced by friction time, the highest yield strength is obtained with the highest friction time which is only 17% compared to 70% for the SS. However, when the friction time increased to the 7 s, failure occurred on the SS side due to the extended deformation and heat-affected zone. If the friction time is held long, a broad diffusion zone with intermetallic phases may be generated. Such parameters as short friction time, low friction and low upsetting pressures will result in a weakly bonded joint. Hence, the quality of the welds strongly depends on the temperature attained by each substrate during the welding process. Therefore, the flow stresses-temperature relationship for each metal will have an important influence on the friction welding parameters. However, it is also reported that. It is also well known that for achieving high strength at welding interface the brittle phases such as σ phase, δ ferrite and oxide formations should be pushed away from the joint surface.

Friction time plays an important role in the flash formation, which gets bigger with increasing friction time on both sides of materials due to the higher heat input and extensive plastic deformation. Thus, the burn-off (axial shortening) increases with the increase of plastic deformation. Two main regions are observed on the welded samples: a dynamically recrystallized zone with extremely fine grains and a plastically deformed heat-affected zone. The width of both zones changes due to the materials properties, i.e. yield strength, coefficient of thermal expansion (CTE), and ductility. Low yield strength, high heat conductivity, and high ductility at elevated temperatures cause more deformation of the AISI 1060 side compared with AISI 304 side. Thus, a more plastic deformation, extended HAZ and more axial shortening were observed on AISI 1060 side and these properties expanded with increased friction time. It is seen that sufficient friction time on the joining surface resulted in an adequate locking of the surfaces, where extensive plastic deformation and microstructural changes occurred, and these facts caused the better tensile response of the joint, where recrystallization occurred on the AISI 1060 side (higher deformation) and grain refinement and strain hardening occurred on the AISI 304 steel side (lower deformation). The width of the recrystallized zone is mainly affected by the friction time. An increase in the friction time results in a wider size of the fine grain region. The change of microstructure and higher axial shortening is also observed in the AISI 1060 side. Heat flow is observed preferentially in the material with higher thermal conductivity. The specific heat was so large, and hence most of the frictional heat generated in the AISI 1060 side. The difference in thermal conductivity explains the microstructural changes, which occur preferentially in the AISI 1060 side. Microstructural changes of AISI 304 side and AISI 1060 side of the weld. During the friction welding process, the temperature near the welding interface reaches just above A1 temperature, which is almost equal to the recrystallization temperature for the steel. Therefore, extremely fine Equiaxed grains formed from ferrite and pearlite. Martensitic structure could also be seen in this region, when the welding interface reaches A3 temperature with the occurrence of rapid cooling. Therefore, the microstructure of AISI 1060 steel turned into austenite. When the austenitic structure was exposed to top cooling from evaluated temperatures, the microstructure turned into martensite due to the diffusion of carbon to the grain boundary and rapid cooling rate. These results mean that the weld experienced

different thermal histories. The relatively quick cooling rate influenced the microstructure of the weld.

[5] studied the effect of burn-off length on the properties of friction welded dissimilar steel bars. Austenitic stainless steel (AISI316L) and carbon steel (SAE1045) materials with dimensions of 16 mm in diameter and 100 mm in length rods were used. Burn-off length1- 6mm were selected and tensile, micro-hardness, and fatigue tests were carried out, besides optical microscope and electron backscattered diffraction analysis were used to characterize the weld interface properties.

The appearance of the weld cross-section from the CS side to the SS side was revealed a large difference in the formation of burrs of the weld flash, which is extruded and plastically deformed from the rubbing surfaces during welding. The amount of plastic deformation on material flow is observed to be more on the CS side compared to the SS side, the difference in decreasing of young's modulus of both the steels at high temperatures leads to the difference in the formation of weld flash. Whereas, grain refinement on the SS side is quite different from the CS side and its width is observed about 100 μm, due to its high resistance to deformation at elevated temperatures. During an analysis of microstructure, which consists of several sub-layers in the interface between the CS matrix and mixed region represents as smooth and planar, whereas the interface of the intermixing region to the SS matrix showed a ragged region with the presence of multi sub layers. This is because of the higher hardenability and lower plasticity nature of the austenitic stainless steel even at high temperatures. It is also observed that these variations are changing with the increasing of burn-off length. The optimal value of a 4 mm burn-off length is determined based on the highest strength of the joints.

While conducting the hardness test of the HAZ the researcher identified an increase of hardness in all parts which were higher than the parent material hardness. Thus, the strength of the parts tends to increase with an increasing burn-off length up to 4mm and decreases gradually up to 6mm.during tensile test of this study the researcher reported that the fracture has occurred in the parent metals in the burn-off length <4 and at weld zone for a burn-off length up >6. In conclusion, the strength of friction welds and width of intermixed zone both increased with increasing of burn-off length up-to 4 mm with a maximum tensile value of 709 MPa and 62 μ; and the maximum hardness values are identified at weld interface and its values varied from 362 Hv to 286 Hv.

Handa and Chawla[9] and [10] performed an experimental study of mechanical properties of friction welded of both similar and dissimilar steel bars. They had prepared a continuous drive friction welding setup using a lathe machine to execute the experiment. In their first study [9], AISI 1021 bars were selected and before the experiment, all needed preparation was done. After that welded joints were subjected to different mechanical tests to determine their best weld quality, reliability, and strength of the weldment. Both axial pressure and rotational speed were the parameters used to investigate the mechanical properties of the welded parts. Thus it was observed Means that the strength increases with the increase in axial pressure up to 120 MPa and then there is a little decrease in strength. The maximum tensile strength of 472 MPa was achieved at the axial pressure of 120 MPa at the rotational speed of 1250 rpm.

In the conclusion of their first study; the production of friction welds was justified to be successful. The mechanical properties of the welds tend to vary with a variation of axial pressure and rotational speed has been the highly influential parameter during the investigation. The hardness of the HAF

increases with an increase of both axial pressure and rotational speed. Thus, it has been found that 1250 rpm and 120 axial force combination were been the parameters to achieve the highest tensile strength.

Whereas, in their second study [10], they had studied the effect of axial pressure on friction welding of austenite stainless steel AISI 304 and low alloy steel AISI in the same setup and preparation as previous. The friction welded specimens of deferent welding combinations were prepared by varying the axial pressures at a constant speed of 1250rpm; it was found that a flash has been produced during the friction welding process and the amount of flash increases with the rise in axial pressure. It has been observed from the experiments that the formation of flash is higher towards the low alloy steel than the austenitic stainless steel in all cases. This might be attributed to the presence of Cr in austenitic stainless steel; as AISI 304 has lower thermal conductivity compared to low-alloy steel, for this reason, the formation of flash is higher on the AISI 1021 side than the AISI 304 side; also austenitic stainless steel has greater hardness at higher temperatures compared to low-alloy steels. For this reason, austenitic stainless steel does not undergo extensive deformation while the low-alloy steel undergoes extensive deformation. During tensile testing, brittle fracture appeared at 75 and 90MPa axial pressures and the joint failed on the weld interface without showing any necking; whereas, at an axial pressure of 105 MPa, the joint also failed from the weld interface but little necking appeared at the interfaces; whereas, cup and cone fractures observed at pressures of 120 and 135 MPa. The tensile strength of these two specimens was found to be very close to the tensile strength of the weaker parent material. This might be attributed to the increase in the axial pressures; more mass in terms of elemental diffusion from austenitic stainless steel to low-alloy steel is thought to be transferred out of the interface due to more friction, thus, increasing the tensile strength. The result depicts that it has also been observed that the maximum hardness was obtained at the weld interface for all the joints the peak hardness of friction welded joins increases with the increase in burnoff length; and with the increase in burn-off length, a soft region appears on the austenitic stainless steel adjacent to the weld interface. The formation of soft regions can be attributed to decarburization; this may be occurred by the presence of heat as the thermal conductivity of the material is relatively low. In addition to that, the higher values of hardness at the weld interface were probably due to the oxidation process which takes place during friction welding. AISI 1021 shows less hardness as compared to the AISI 304. This decrease in hardness may be attributed to the recrystallization process taking place at the heat affected zone towards the low-alloy steel. On the study of friction welding of nickel-free high nitrogen steel: influence of forge force on microstructure, mechanical properties and pitting corrosion resistance[11] CDFW machine with a capacity of 150 KN was used to execute the experiment. Friction force of 20 KN, forge force ranging from 20KN-60 KN, and burn-off length of 5mm was used; whereas the other parameters such as rotational speed were kept constant. The joint characterization studies include microstructural examination and evaluation of mechanical (micro-hardness, impact toughness and tensile) and pitting corrosion behavior was studied. It was reported; the continuous drive friction welding machine was able to create defect-free weld joint of high nitrogen steels, Welds exhibit poorer Charpy toughness and tensile strength than the base material. Thus, Toughness value for the welds goes down with an increase in forge force, Welds show poorer than the base material whereas the forge force does not affect the tensile strength of the welds. But, Pitting corrosion resistance of friction weldments is

much lower than that of the base material. It decreases with an increase in forge force.

[12] studied the Effect of Interlayer in Friction Welding for Dissimilar Steels: SS 304 and AISI 1040 by using nickel interlayer a compare quality of the weld with and without an interlayer. Forging pressure, rotational speed and friction time were the three parameters used to carry out experiments. Taguchi orthogonal array was used for designing the experiment and optimization of experimental results has been done (L9 orthogonal array for 3 parameters and 3 level using Minitab). From the main effect Plot for SN ratios the optimized parameters for maximum tensile strength for weld with interlayer and without interlayer were speed 2200 rpm, forging pressure 1.570 ton, burn off length 8 mm and speed 2100 rpm, forging pressure 1.884 Ton and burn off length 4 mm respectively. It is exhibiting a fine microstructure at the SS304 side when the interlayer is introduced. The frictional heat generated during the rubbing of the two mating surfaces at the interface is expected to deform the SS304 side which along with the combined effect of higher forging pressure and burn off length exhibits a fine microstructure in the zone. Also, the thermal conductivity of AISI 1040 is more than that of SS304, thus the formation of heat at the interface by friction effect might have contributed mainly to the SS304 side because of its lower conductivity.

During testing the strength of the welds Failure location matched with the minimum hardness region. The UTS of the final weld without interlayer is 630MPa which is approximately equal to the value obtained by optimization using Minitab (636MPa) and ultimate tensile strength of the final weld with nickel as interlayer is 656MPa which is closer to the value obtained by optimization using Minitab (661Mpa). This increase in strength can be accounted primarily to the presence of nickel which reduces the formation of inter-metallic in the weld region, also the higher burn-off length when using interlayer decreases the inter-metallic and plastically deformed regions which are expected to result in higher tensile strength. The microhardness value reached a maximum at the interface. The increase in hardness at the welding interface is probably due to friction and oxidation processes which takes place during welding processing and also may be due to the formation of brittle inter-metallic which is one of the reasons for lower tensile strength for weld without an interlayer, but the hardness tends to decrease for weld where the interlayer is used, this can be accounted to the presence of Ni in the interface. During welding, Ni reduces the precipitate on of chromium carbide. Nickel also accounts for the reduction of soft regions near to the interface which in turn reduces the hardness.

The current study is more complicated because burn-off length has also been varied here and there could be a combined effect of variation of friction pressure and burn-off length. [13] statistical analysis of rotary friction welding of steel with varying carbon in workpieces were studied in continuous drive friction welding on materials that comprise both the same and different carbon contents. Variations of strength and hardness of welded parts were examined. The parameters used during experimentation were rotational speed, forging pressure and carbon content whereas keeping other parameters constant. Experimental results were analyzed and optimized using response surface method. During examining the tensile test results by response surface method, the ANOVA results implied that the suggested model was linear and the model was significant with its prob>F value 0.0003 which were < 0.05 and A, B, C were the significant model; but, the lack of fit was significant which means the predicted R2 was not in good agreement. the predicted R^2 was found to be 0.477034 which was in good agreement with the adjusted R^2 but in response surface method the predicted R2 has to be above 0.9 and the adjusted R^2 should have to be greater than that of predicted

R^2 .Whereas the increase in the hardness of the HAZ was also analyzed and the model suggested were linear model and the model probe>F=0.001 and lack of fit probe>F= 0.0984; which implies that the model is significant because it was <0,05 and the lack of fit is insignificant, means the predicted R^2 (0.871699) was with great with its adjusted R^2 (0.898176). The statistical results were validated, confirmed and optimized by response surface method. The optimization was carried out with targets of maximizing the strength and minimizing the variation of hardness. In conclusion; all the parameters had significant effects on the tensile strength of the weld interface, and it increases gradually with the increase in values of the parameters. Both forging pressure and carbon content tend to affect the hardness of the HAZ, but the carbon content of the material affects the HAZ than the forging pressure relatively. Whereas, at low carbon content, the forging pressure increases the harness and carbon content < 20% and > 40% don't have an imminent effect in the hardness. In addition to that more than a hundred percent strength of the parent material had been found in the weakest material. [14] in their study entitled an analytical study of dissimilar materials joint using friction welding and its application used SS316 and EN8 for experimentation with parameters such as rotational speed, friction time, forging pressure and friction pressure and the tensile strength of the samples were examined. A partial factorial design of experiment based on Taguchi analysis was conducted to obtain the response measurements. Analysis of variance ANOVA and main effects plot was used to determine the significant parameters and set the optimal level for each parameter. Based on the experimentally determined optimal parameters a confirmation experiment is conducted. 3 level 3 factor design was selected which was L9 (3x3) orthogonal array, thus 9 number of runs were carried out. The controlled factors used were; rotational speed, forging pressure and cooling medium and the response variable was tensile strength.

It has been observed that the friction processed joint exhibited good strength and joint strength increased with increase in friction pressure and forging pressure at high and moderate levels of rotational speeds and the optimal value of process variables for a higher tensile strength from the Taguchi design is 1580 R.P.M, 28 bar forging pressure and oil quenching. A study of the regression analysis for tensile strength was also studied and the correlation between experimental values and predicted values of tensile strength was established with a correlation coefficient of 0.971. The main effect for SN ratio and the relation between parameters by employing ANOVA was studied for Tensile strength of the joint; and it was observed that at all levels of variables, there is an interaction between control factors and the response variable and the contribution of the interaction between control factors is negligible. And from the main affects plot the level of factors that have more effect on the tensile. From the Taguchi design of the experiment it is observed that the factor that has more effect on the Tensile Strength is forging pressure then speed and finally cooling method.

[15] studied Mechanical Properties of Dissimilar Friction Welded Steel Bars solid bar chrome-molybdenum steel (SCM440) to carbon steel (S45C) not only to optimize the friction welding conditions but also to investigate the fatigue performance. Tensile tests, Vickers hardness surveys of the bond of area and HAZ, and microstructure investigations evaluated. Preliminary welding trials were carried out to determine the welding conditions. During these studies, the rotating speed was maintained at 2,000rpm. The study led to the following conditions being selected; heating pressure 60MPa, upsetting pressure 100MPa, and heating time 1-7 sec. For friction welded connections of SCM440 to S45C steel bars, the total upset increases linearly with increasing the heating time.

Optimal welding conditions were selected as follows; rotational speed 2,000rpm, heating pressure 60MPa, upsetting pressure 100MPa, heating time 4second, upsetting time 5second and total upset 5.7mm. The weld interface of dissimilar friction welded steel bars is mixed strongly, and the heat-affected zones of the center line and circumferential line are about 5.3 and 6.0mm, respectively. The Vickers hardness of the friction weld interface is 2 times higher than that of base metal. As a result of observing the microstructure in the welded part (welded frictionally in the optimum condition stated in this research), two different kinds of materials are strongly mixed to show a well-combined structure of micro-particles without any molten material and particle growth or any defects. Finally, the mean S-N curve representing the as-welded notched specimens tested appeared significantly higher than the base metals. [20]they have studied the effect of welding parameters on the fatigue properties of dissimilar AISI 2205 – AISI 1020 joined by friction welding both the dissimilar bars were connected using different operating parameters. Tension test and rotary bending fatigue test were applied to the welded connections, and the impact of the welding parameters on fatigue strength was examined. Successful weld joints that inherited greater strength from the parent material were found to be 633,790 Mpa and the parent material was found to be 610.780 Mpa. The highest fatigue limit was achieved in friction time of 4s and a lower fatigue limit was achieved in 8s. Thus it was reported that both tensile strength and fatigue limit decreases in increasing friction time. Therefore, it had been determined that a better connection quality can only be obtained by selecting the parameters (rpm, friction time, accumulation pressure and accumulation time) to comply with each other.

AISI 304 has been studied by various researchers in joining it by rotary friction welding with different steel bars which constitute different chemical composition. It was also joined with nonferrous metals; such as aluminum. But, never been joined with a AISI 4130 low alloy steel. Owing to the abundance of AISI 4130 in our environment due to their low cost expenses and their wide range application of austenite stainless steel this current study emphasizes in joining dissimilar steel bars (AISI 304H and AISI 4130) using CDFW setup lathe machine. In this current study; prior to experimentation numerical analysis has been carried out in order to be validating by experimental results. Working temperature of the CDFW welded parts were been recorded by infrared thermometer for validation of the numerical temperature distribution results. In addition to that, tensile, micro-hardness, and microstructure of the welded parts has been examined and an optimization was executed by design expert software in a response surface method

3 METHODOLOGY

In this study, the following materials and apparatuses were used

3.1 ***Materials***

The materials used in this research are AISI 304H and AISI 4130 bars of diameter 12mm and length of 153mm.

3.2 ***Apparatuses***

- **Spectrometer**:- used to identify the chemical composition of the parent materials
- **Etchant**:- cleaned the specimen prepared for microstructural and hardness
- **Hack saw**:- cut the specimens to the desired length
- **Infrared thermometer**:- measured the working temperature during the experiment
- **Stopwatch**:- to record the friction time of the experiment
- **Tensile testing machine**:- examined the tensile strength of the rotary friction welded bar
- **Hardness testing machine**: - used to examine the hardness of both the welding zone of the materials and the inherent materials.

3.3 Research Design

Fig. 3.1: Research design flow chart

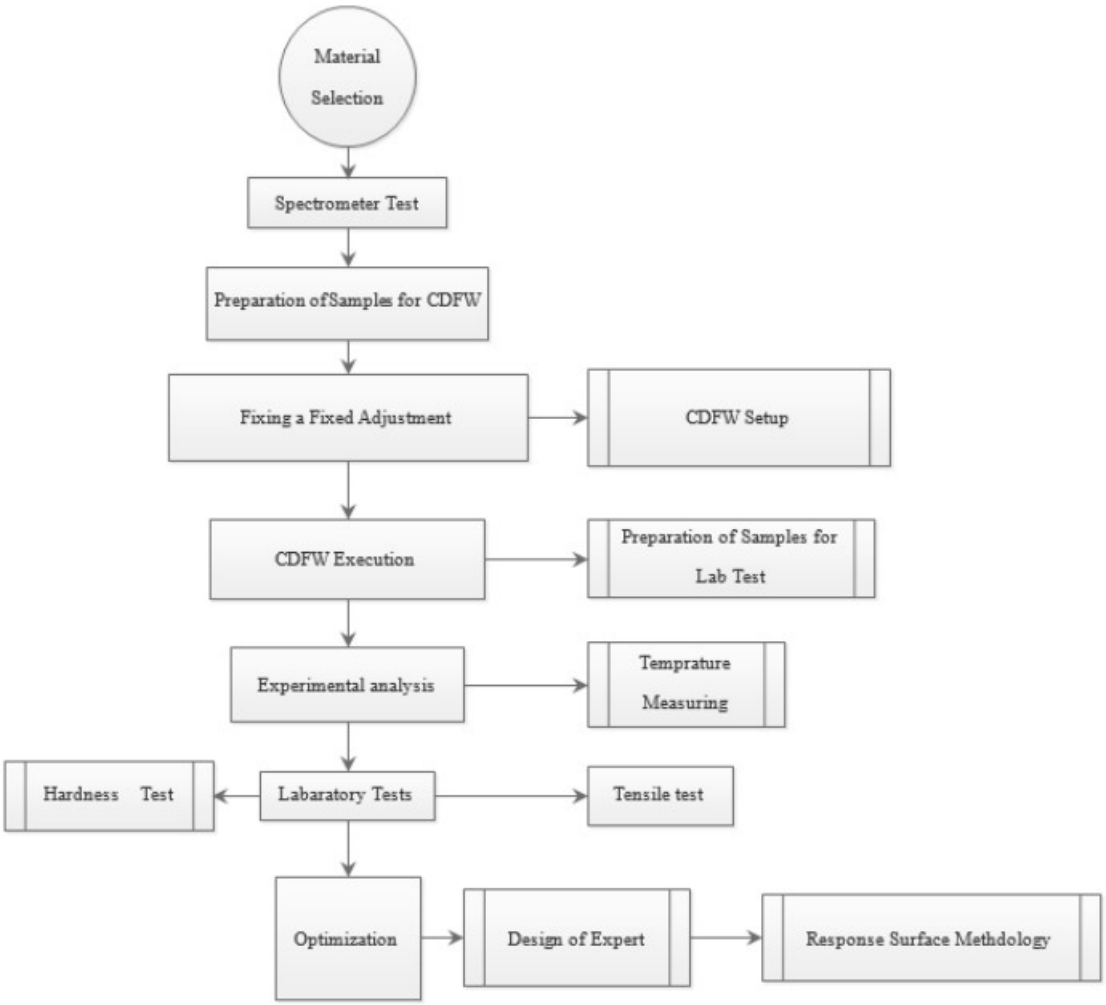

3.3.1 Spectrometer testing

Fig. 3.2: **Spectrometer testing tools**

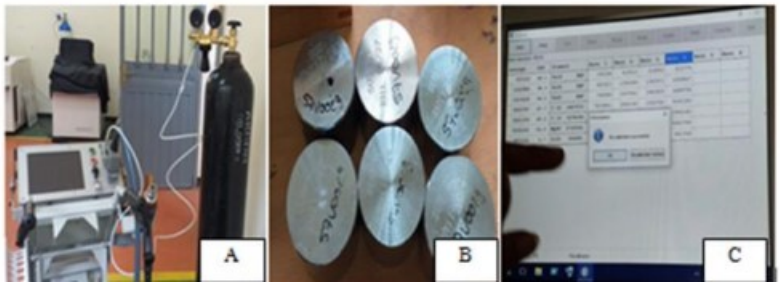

(A) : Oxford spectrometer with its argon gas cylinder, (B) : Recalibration blocks, and (C) : Recalibration success

Sample Preparation

The most critical part in chemical composition examination is preparing a sample: because the quality and reliability of the analysis depend on it. Since the spark discharge only evaporates material on

the surface and does not penetrate deep into the material, it also measures all the impurities on the surface. Dirt, oils, oxides, and even fingerprints can disturb analysis and prevent the formation of plasma. In that case, it'll obtain a poor burn spot with very low luminous efficacy ("white focal point"). The result is a faulty analysis that means the analyzed sample composition does not correspond to the actual composition. See page 22 Figure 3.3 for details

Fig. 3.3: Start and sequence of check measurement in spark mode

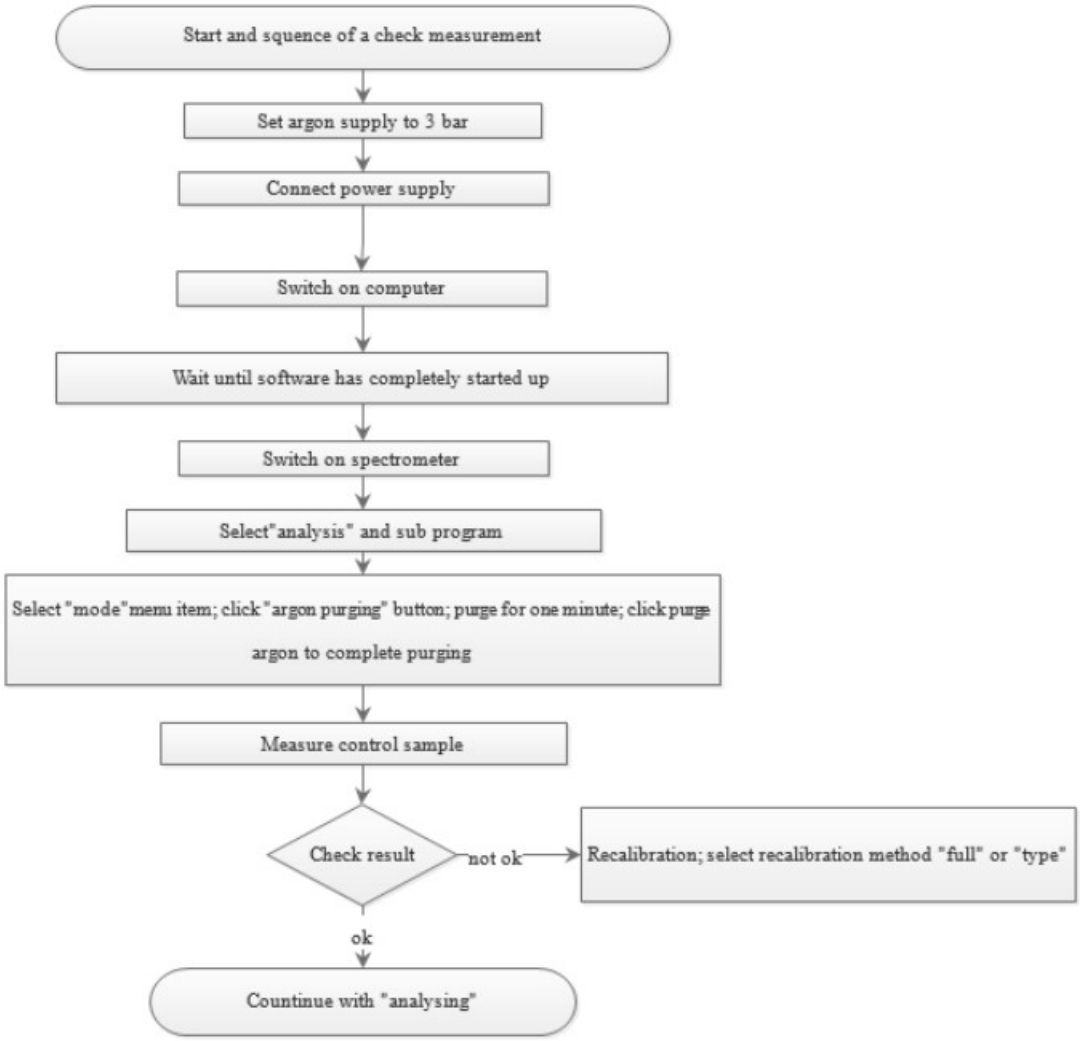

Fig. 3.4: Prepared samples for spectrometer testing

(A) : Low alloy steel (4130) and (B) : Austenite stainless steel (304H)

Tab. 3.1: Comparison of chemical composition (%) of AISI 304H

Grade AISI 304H		C	Mn	Si	P	S	Cr	Mo	Ni
Theoretical result	**Min**	0.04	-	-	-	-	18.0	-	8.0
	Max	0.10	2.0	0.75	0.045	0.030	20.0	-	10.5
Lab result	**Max**	0.10	2.0	1.0	-	-	20.0	-	12.0
	Min	0.030	-	-	-	-	18.0	-	8.56

Tab. 3.2: Comparison of chemical composition (%) of AISI 4130

Grade AISI 304H		Cr	Mn	Mo	P	S	Si	C
Theoretical result	**Min**	-	-	-	-	-	-	-
	Max	1.00	0.80	0.20	0.04	0.04	0.30	0.30
Lab result	**Max**	1.10	0.70	0.25	-	-	0.50	0.350
	Min	0.80	0.40	0.15	-	-	0.30	0.25

3.3.2 ***Continuous Drive Friction Welding Setup***

Continuous Drive Friction Welding is a variation of friction welding in which the energy required to make the weld is supplied by the welding machine through a direct motor connection for a preset period of the welding cycle. In Direct Drive Friction Welding, one of the workpieces is attached to a motor-driven unit while the other is restrained from rotation. The motor-driven workpiece is rotated at a predetermined constant speed. The workpieces to be welded are forced together and then a friction welding force is applied. Heat is generated as the faying surfaces (weld interfaces) rub together. This continues for a predetermined time, or until a preset amount of axial shortening (upset) takes place. The rotational driving force is discontinued and the rotating workpieces is stopped by the application of a braking force. The friction welding force is maintained, or increased, for a predetermined time after rotation ceases (forge force).

CDFW Welders use AC or DC variable speed drives that eliminate clutches and brakes. Proportional hydraulic controls guarantee smooth up and down force control. Through manipulation of deceleration times and forge force ramp-up time, welds can be made ranging from near Inertia Friction welds to classic Direct Drive Friction welds. Rotary friction welding has the inherent limitation that it cannot be used for non-circular cross-section components. Another main disadvantage is that the rate of heat generation is not uniform over the interface ecause of the linear variation of rotational speed with radial distance. This creates a non-uniform thickness of the heat-affected zone (HAZ) across the interface.

Preparation of a Fixed Part

As manifested in the title, this study is performed in the lathe machine Figure 3.5 because the energy required to make the welds came directly from the motor of the lathe machine. Unlike the CDFW machine which uses a DC or AC variable speed drives that eliminates the clutches and brakes which helps the CDFW machine to halt immediately after the desired sample is prepared within the desired independent variables. In this case, the lathe is expected to cease rotating by the use of brakes; so that, the inertia which objects halting the lathe machine needs an extended study, and the parameters included in this study are; rotational speed, friction time, and burn off length: though studying other parameters is possible by additional set up.

Though this sort of welding requires rotating and non-rotating parts, thus, a fixed part that can hold one part stationary was prepared as seen Figure 3.5. The stationary part contains four bolts that can hold the stationary part firmly and the bolts tip were tapered in to maximize the pressure-induced in the stationary part.

Fig. 3.5: Lathe machine used for experimentation

Fig. 3.6: Stationary arrangements of newly CDFW set up in lathe machine

3.3.3 ***Sample Preparation***

The samples were prepared in a dimension of 153mm each in to resemble ISO-6892-1standard to fit exactly the EN-02-metallic materials tensile test-2. During preparation, when the raw material was bout from a local market it was cleaned and cut into a desirable dimension, meanwhile the surface area which is brought in to contact during friction welding was faced (proper allowance were taken in case) in the lathe machine and properly cleaned; even though the process is not affected by dirt, oil, surface scratch, and other impurities; because the process squeezes out these impurities in the form of flash before melting temperature of the parent material.

Fig. 3.7: prepared samples prior to welding

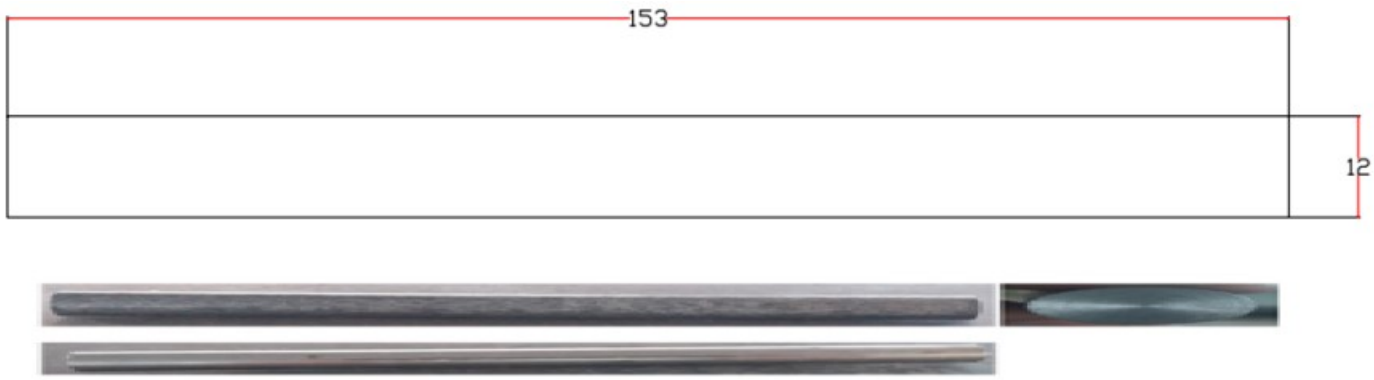

3.3.4 ***Experimentation Execution***

Sample Preparation

Fig. 3.8: Steps followed during experimentation

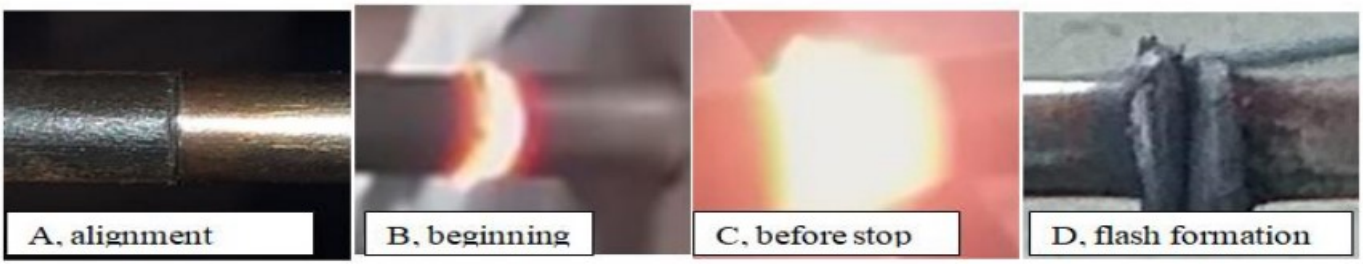

Fig. 3.9: CDFW samples

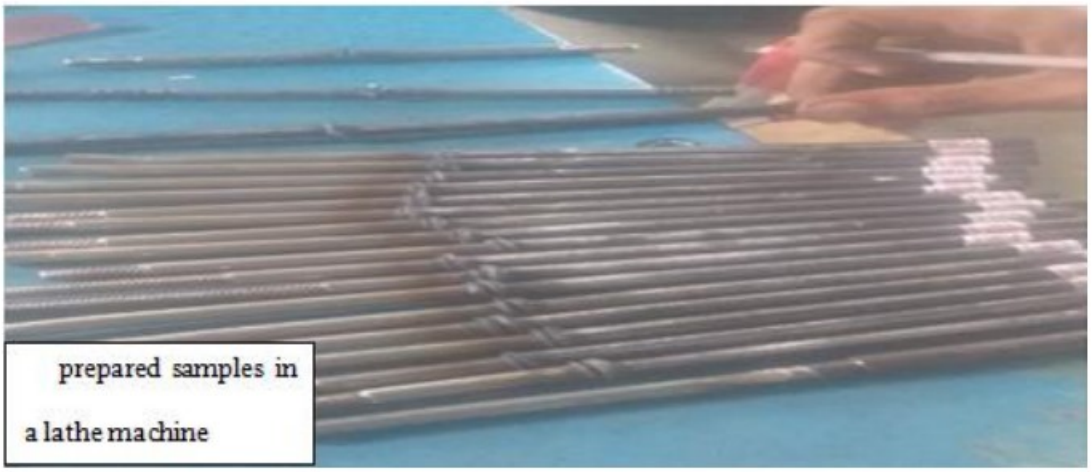

One of the spacemen was fixed into the fixed arrangement, the sample is arranged in the lathe tailstock as a dead center, and the other sample was also inserted into the chuck as a rotating part. Then the samples were brought in to contact, meanwhile the motor start and the chuck which holds the rotating part and the parts start to rub the stationary part and the parts start heating into a specified temperature and the maximum temperature was measured by an infrared thermometer. After a predetermined time the rotation of the chuck was halted whereas the flash of the welded parts were removed after welded parts.

Measuring Temperature

In this phenomenon, a non-contact temperature measuring apparatus was used to measure the working temperature of the experimentation. The thermometer was held firmly by pointing the infrared rays from a possible nearest and safest distance into the welded interface of the parts, thus the maximum temperature was recorded.

Fig. 3.10: Way of measuring temperature

3.3.5 ***Laboratory Tests***

Micro-Hardness test

Before forthwith, a sample of 10 mm from each side of the welded areas was prepared. And the circular area war changed into a smooth rectangular area by a surface grinding in order to suffice the diamond indent used to test the Rockwell hardness of the welded materials. The Hardness of each welded material starting from the welding interface was measured, and five test results were recorded from both sides.

Fig. 3.11: Hardness measurement tools

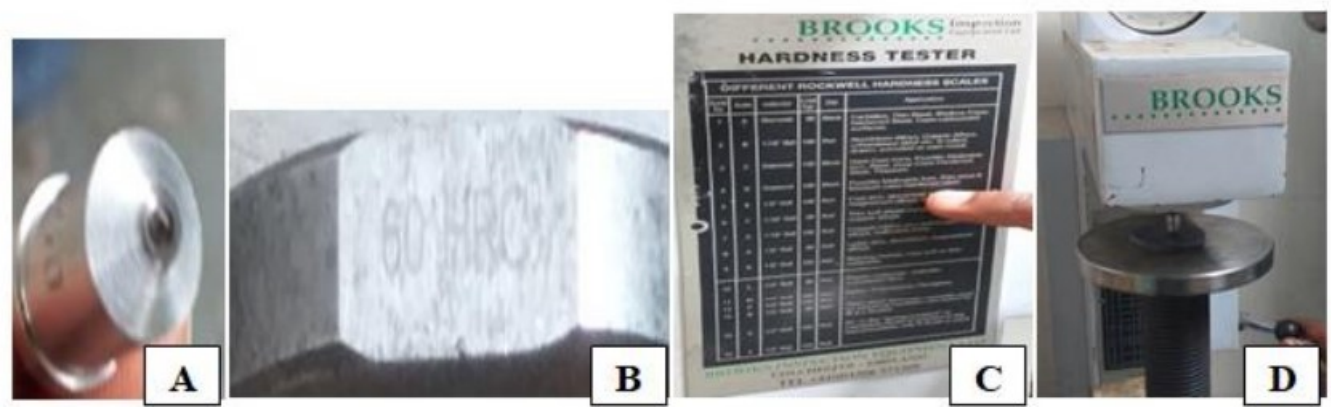

Tab. 3.3: Hardness measurement standards

Testing type	Standard	Description		Industry
Rockwell hardness(HRC)	ISO/6802	**Load** **Indenter type** **Scale**	150 Kg Diamond C	MIDI,Addis Ababa,Ethiopia

Sample preparation: having prepared long circular sample, that makes the measurement of micro-hardness of the parts difficult, because of its circular shape that tends to slip while measuring it. Due to that reason, a new sample was prepared to suffice the indenter. First, the experimental prepared sample was cut in at least ¿10 mm length, and machined into rectangular shapes using surface grinding afterward.

Fig. 3.12: Type of sample prepared for micro hardness test

Tensile Testing

Tab. 3.4: Hardness measurement standards

Type of test	**Type of testing Machine**	**Standard**	**Industry**
Tensile	Universal Tensile Test Machine	ISO/6892-1	Federal technical and vocational education training(FTI),Addis Ababa,Ethiopia

Fig. 3.13: Tensile testing machine

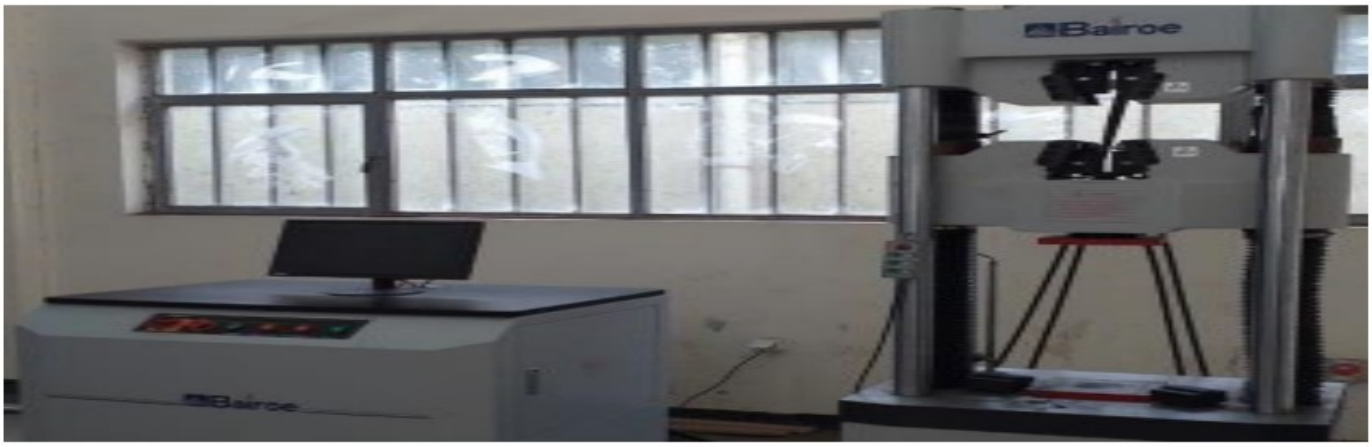

Sample preparation: the following table and figure illustrates the tensile testing standards and sample prepared accordingly.

Tab. 3.5: Dimensions for tensile test standard

Sample diameter(mm)	Cross-sectional area(mm^2)	Grip-grip length(mm)	Original(gauge length(mm))	Total length(mm)
8 mm	50.27	Lc=10d	5d	LT=Lc+220

Fig. 3.14: Sample for tensile test

4 RESULT and DISCUSSION

4.1 Results

4.1.1 Tensile Test Results

As shown in page 28, Table 4.1 the following results were been conducted during experimental execution which also comprises the nominated factors and levels.

Tab. 4.1: Screened number of experimentation and their output

Number of runs	Factor-1(Rotational speed) Designation-A Unit-Rpm	Factor-2(Friction time) Designation-B Unit-S	Factor-3(Burn-off length) Designation-C Unit-mm	Response-1(UTS) Designation-UTS Unit-Mpa
1	700	7	2	350
2	900	7	4	450
3	700	4	2	305
4	700	4	4	329
5	900	10	2	392
6	1120	7	2	530
7	1120	4	2	505
8	1120	10	4	545
9	900	7	4	469
10	1120	4	4	498
11	900	4	3	428
12	900	4	3	435
13	1120	7	3	560
14	700	10	3	38

Effect of Rotational Speed in UTS

As seen in page 29,Figure 4.1, the ultimate strength increases when the rotational speed is enhanced regardless of other factors. As the rotational speed gets higher the produced heat tends to increase, but the produced heat during experimentation is not only dependent on the rotational speed; it also depends on the friction time taken during the welding phenomenon. And the same issue has been reported in [1]. Due to the reason that the rotational speed of the lathe machine is the source of the mechanical energy which thereby changed into thermal energy by the rubbing effect of the rotating and stationary parts of the CDFW which made the heat input due to rotation is constant until the

process is halted. Thus, the results of this research tend to suffice this reason that it has been found both the minimum and maximum value of UTS (305,560) was found in the minimum and maximum input independent variable of the rotational speed (700,1120).

Fig. 4.1: Correlation graph between rotational speed and UTS

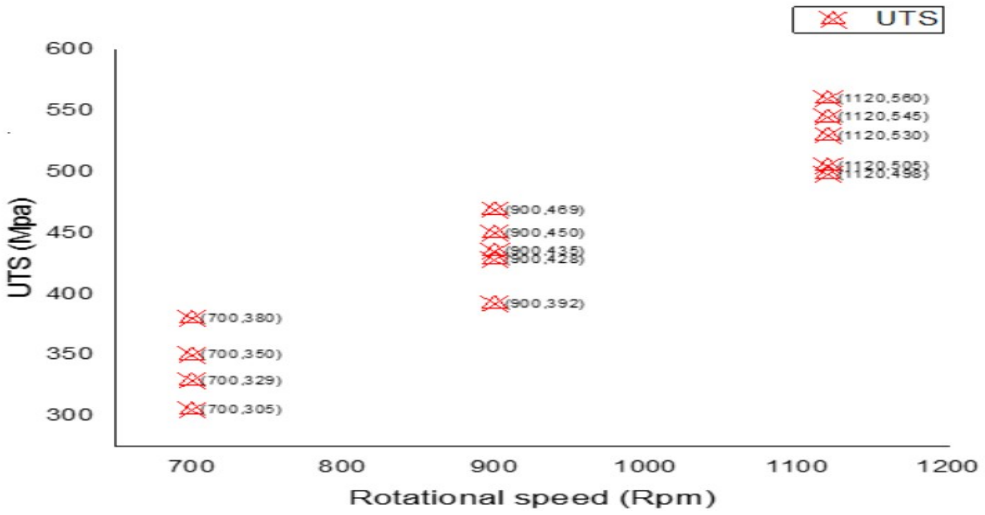

Effect of Burn-off Length in UTS

By visual examination, two main regions are observed on the welded samples: a dynamically recrystallized zone with extremely fine grains and a plastically deformed heat-affected zone. The width of both zones changes due to the materials properties, i.e. yield strength, coefficient of thermal expansion (CTE), and ductility. Low yield strength, high heat conductivity and high ductility at elevated temperatures cause more deformation of the AISI 1060 side compared with AISI 304 side As seen in the above graph, the maximum tensile strength found has 3mm burn of length, but when the burn off length tends to increase the UTS tends to decrease regardless the effect of other factors. This is due to the inclusion of brittle intermetallic in the interface of the weldment. This reason has been backed up by [4]. It is also reported that a good strength can be obtained by a sufficient diffusion and mechanical locking [8], thus proper locking has been achieved especially in burn off length 3 and less amount of tensile strength was obtained in 2mm burn off length due to lack of proper diffusion and leftover impurities in the welding interface. It is also observed that the range of burn-off length between 2 mm and 3 mm was revealed a good amount of ductility for the friction welded joints. The strength of joints gradually increased with increasing of burn-off length up to the optimum level and starts to decrease after reaching its optimum value of 3 mm bun-off length. It has been reported in [10]

Fig. 4.2: Correlation graph between Burn-off length and UTS

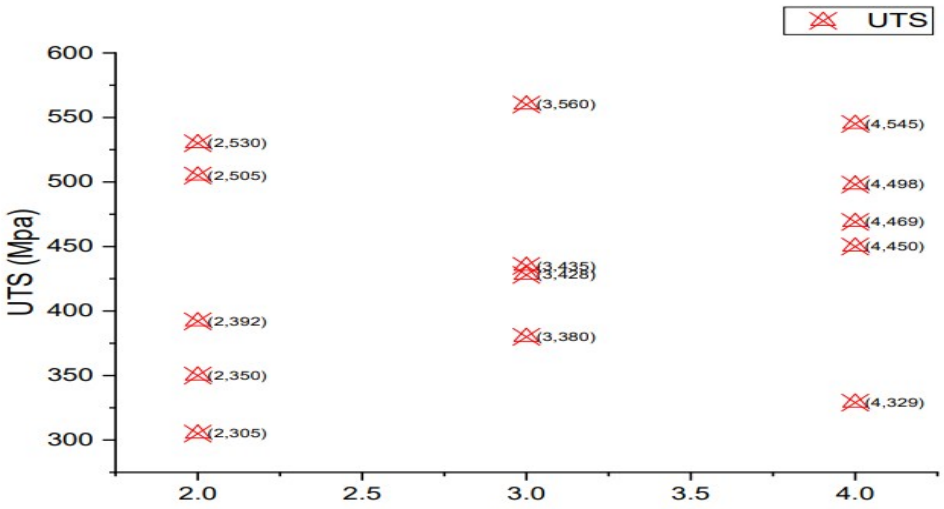

Effect of Friction Time in UTS

Change of friction time results in a change in the welding strengths of the joints which are related to the produced and useful heat variations in friction welding. For the lower values of friction time, welding strength decreases due to a decrease in heat acquired in the welding interface. Higher tensile strength was found in friction time of 7s and lower tensile strength was found when the friction time was less or greater than seven seconds. Due to the reason that welding strength reaches a maximum in an increased amount of friction time and turns down beyond the maximum point, because produced heat causes regional melts that decrease the welding strength when he welding phenomenon stays longer time and the same reason has been reported in [1], and [33]. In addition, time plays an important role in flash formation, which gets bigger with increasing friction time on both sides of the materials. If the friction time is held long, a broad diffusion zone with intermetallic phases may be generated. Thus, the quality of the welds strongly depends on the temperature attained by each substrate during the welding process. Therefore, the flow stresses-temperature relationship for each metal will have an important influence on the friction welding parameters. In the long-time welding, the heating time was prolonged to increase the maximum temperature at the weld interface, to increase the time for axial conduction of heat into the two work pieces and to decrease the subsequent cooling rate

Fig. 4.3: Correlation graph between Friction time and UTS

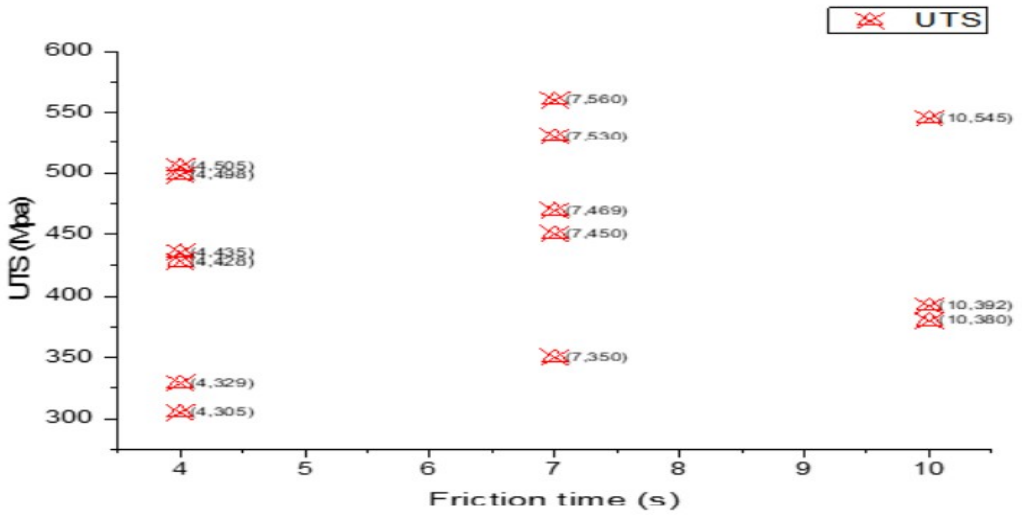

Effect of All Combined Parameter in UTS

As seen in page 31,Figure 4.3, the least tensile strength was found in run number 3 where all the factors are in their very least (700,4,2). It has been reported in [6] that proper forging and heat input is required to create a fully intermixed bond between the weld and to push out the flash that contains a ferrite brittle materials. The tensile strength increases at increasing friction time and burn off length up to some level then declines when it reaches burn off length and friction time 4 and 10. But, it increases intermittently when the rotational speed increases up to the maximum level. At higher rotational speed, time plays an important role in flash formation, which gets bigger with increasing friction time on both sides of materials due to the higher heat input and extensive plastic deformation. Thus, the burn-off (axial shortening) increases with the increase of plastic deformation. If the friction time is held long, a broad diffusion zone with intermetallic phases may be generated. Such parameters as short friction time, low burn-off length and low rotational speed will result in a weakly bonded joint. It is also well known that for achieving high strength at welding interface the brittle phases such as $\sigma - phase, \delta - ferrite$and oxide formations should be pushed away from the joint surface. In this case, to achieve higher strength, the friction time and upsetting length should be as high as possible for the pre-specified rotational speed. As the friction and wear help to get rid of contaminants like oxide on the interface, a new face should be surfaced. At the same time, the upsetting and friction pressure and friction time set in to bring the new face within the scope of attraction range. The visual inspection of the fractured parts revealed that most of the specimens were failed at the weld interfaces and brittle fracture appears to occur. The same issue has been encountered in [9].

Fig. 4.4: Correlation graph between burn off length and UTS

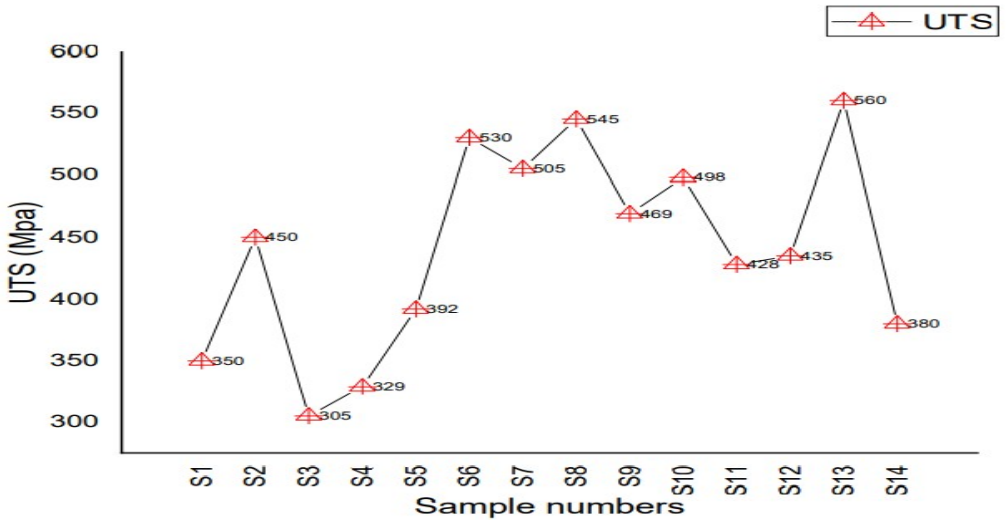

4.1.2 ***hardness Test Results***

Continuous drive friction welding process increases the hardness values due to heating and cooling effects. Hardness values that are equal to the normalized hardness of test material are raised to higher levels by the process within the HAZ. Therefore, maximum hardness values are obtained over the weld interface. The hardness values generally increased with increasing friction time and upsetting length. The increasing hardness values in the welding interface can be related to the microstructure formed in the joint surface as a result of the heat input and extensive plastic deformation. It can be said that microstructural evaluations around the interface, diffusion of elements on the sides, work hardening, dislocation density, grain refinement, and formation of precipitations may have caused this increase. Although the work hardening is also effective on the hardening in AISI 304 side, much of the hardening in AISI 1060 steel is a direct result of fine grains, formation of precipitates and rapid cooling from the welding temperature.

Tab. 4.2: Hardness measurement standards

Run no	Factors(A,B,C)	Distance from interface of the weld zone(mm)											UTS(Mpa)
		AISI 304H								AISI 4130			
		-10	-8	-6	-4	-2	0	2	4	6	8	10	
3	700,4,2	21	21.5	22	23	25	26	24	22	21	19	17	305
4	700,4,4	21	22	23	25.5	27	29	26	25	22	20	18	329
5	900,10,2	22	23	24.5	25	26	28	25	23.5	22	20.5	18.5	392
9	900,7,4	22	24	26	27.5	29	32	29	27	25.5	24	21	469
10	1120,4,4	21	24	26	29	30.5	33	28	27.5	25	22	17	498
13	1120,7,3	21	22	23	24	25.5	26	24	22.5	19	18.5	17	560

(A) rotational speed (B) friction time (C) burn off length

In the literature, a similar hardness profile was also observed for dissimilar material couples [5, 6, 9, and 10]. It can be said that the hardness properties are influenced by an interactive effect of friction time and burn off the length which are combinations of heat input, range of plastic deformation and degree of strain hardening. The influence of the welding parameters on the horizontal hardness distributions is shown in the figure shown below. Both sides of the materials are hardened due to the transformation of austenite to the martensite, which is strongly affected by the cooling rate.

Six samples were been investigated in the below three figures in order to see the hardness variation in the HAZ and see the relationship of the increased hardness and decreasing tensile strength of the

welds. It was found that in a maximum hardness of samples 3, 4, 5 was 26, 29, 28 HRC respectively and UTS of 305, 329, and 392 Mpa respectively.

Fig. 4.5: Hardness variation across HAZ distance Sample 4 and 9

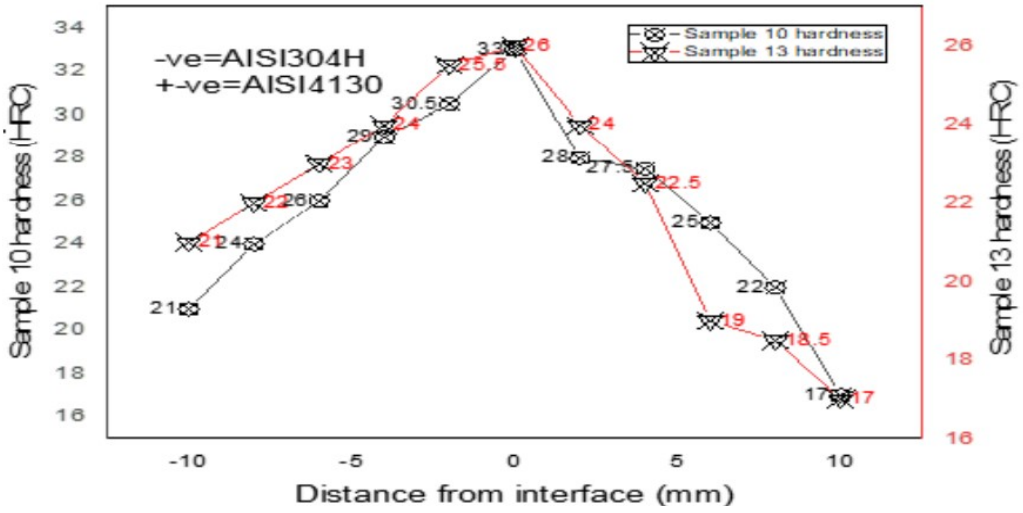

Fig. 4.6: Hardness variation across HAZ distance Sample 10 and 13

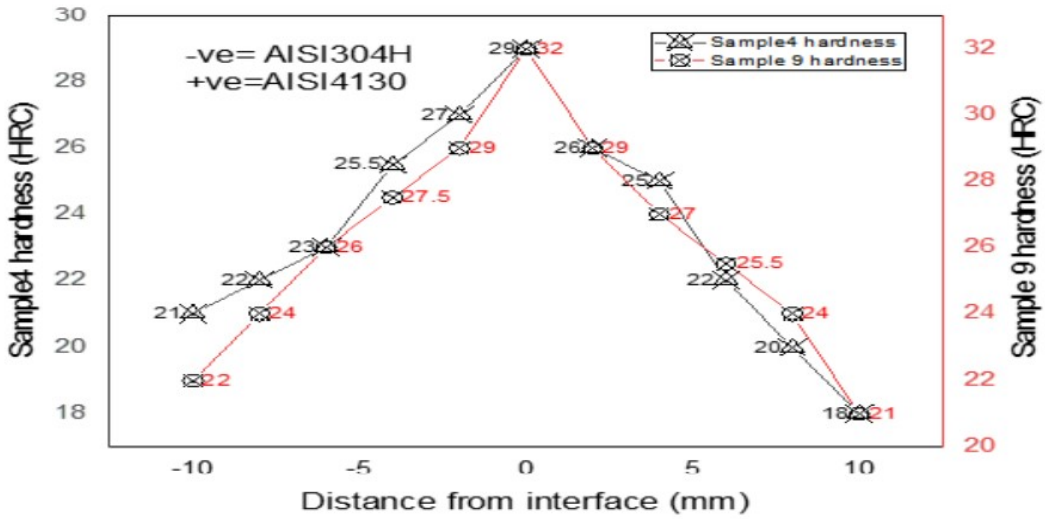

Fig. 4.7: Hardness variation across HAZ distance Sample 3 and 5

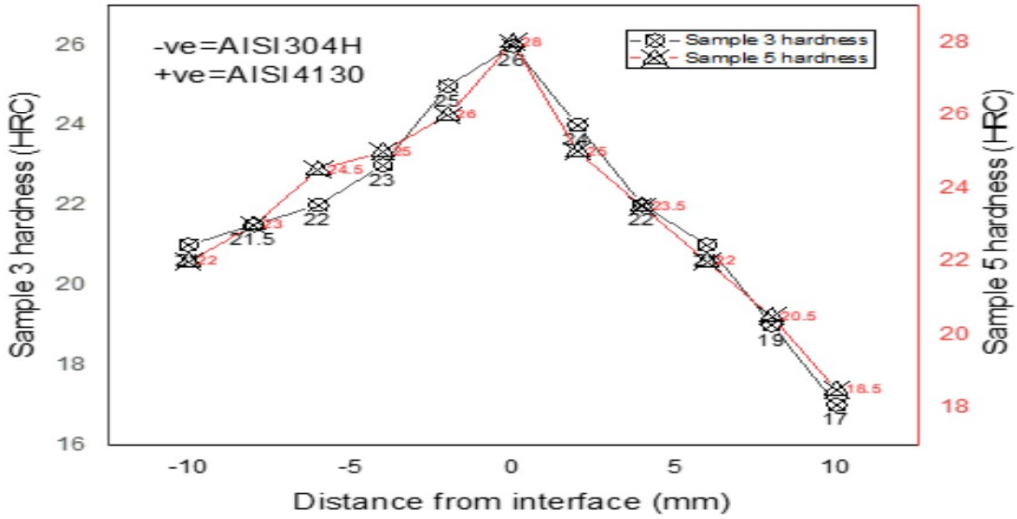

The UTS tends to decrease when the hardness of the weld interface increases. It is also evident that the hardness value increases where there is a greater rotational speed and burn off length.it was reported [6] formation of mixed layers in the joint interface could be one of the reasons for the reduction in joint strength. The correlated value of the width of the mixed region to the tensile strength and width of the mixed region to the burn-off length confirms the effect burn-off length on the joint properties.

The hardness distribution varying within the mixed region from 29 HRC to 21 HRC from the AISI304H side and 29 to 17 HRC from AISI 4130 side this is as seen in all figures from below. The distribution of the hardness across the HAZ has been measured horizontally till 10 m away until it was reached the parent material hardness. As seen in the figure below the hardness variation tend to increase as the measurement tends to approach the interface of the welded parts and it decreases when the measurement was from the interface into the parent material till it reaches the hardness of the parent material. The below-plotted graph implies Burn-off length is the axial shortening of the length during friction welding and it was observed that with the increase in burn-off length, a soft region appears on the AISI 4130 adjacent to the weld interface. The formation of the soft region can be attributed to decarburization. This may be occurred by the presence of heat as the thermal conductivity of the material is relatively low. In addition to that, the higher values of hardness at the weld interface were probably due to the oxidation process which takes place during friction.

The above Figure 4.5,4.6, and 4.7, page 33 testifies that the reasons explained above to be true by the results demonstrated above. The highest hardness was found in samples 13, 10 which were 33 and 32 respectively and the combination of factors were 1120, 4, 4 and 700, 7, 4. In the first case, the rotational speed and the burn of length were at their maximum; thus a proper plastic deformation has been taking place that leads to carburization and oxidation; hence decreases the strength of the welding parts. In the second case, even though the burn-off length has been kept at its maximum but the rotational speed which was the source of the heat was decreased and the friction time was enhanced to acquire proper heat in the welds. Thus a higher amount of hardness variation has been obtained which leads into decreasing of the strength of the welds.

4.1.3 ***Temperature Test Results***

As shown in Table 4.3; the temperature of each experiment was recorded by infrared thermometer, and their effects on the hardness, and the quality of the weld are investigated.

Tab. 4.3: Experimental temperature results measured by infrared thermometer

Number of runs	Factor-1(Rotational speed) Designation-A Unit-Rpm	Factor-2(Friction time) Designation-B Unit-S	Factor-3(Burn-off length) Designation-C Unit-mm	Experimental Temperature Unit-^0C
1	700	7	2	352
2	900	7	4	481
3	700	4	2	309
4	700	4	4	318
5	900	10	2	504
6	1120	7	2	564
7	1120	4	2	539
8	1120	10	4	615
9	900	7	4	485
10	1120	4	4	548
11	900	4	3	459
12	900	4	3	452
13	1120	7	3	572
14	700	10	3	379

Effect of Temperature on the Strength of the Weldment

As shown in Figure 4.8, the UTS increased as the temperature increased as well. The temperature plays an important role in CDFW that the better the temperature the better the coalescence of the weldment and it also creates a better interlocking of during an intermetallic formation. The case is not always true because, sometimes an excessive temperature might encounter nearly melting or above recrystallization temperature which makes the weldment weak and very wide HAZ can be formed which undesirable in this case.

Fig. 4.8: Temperature vs UTS graph

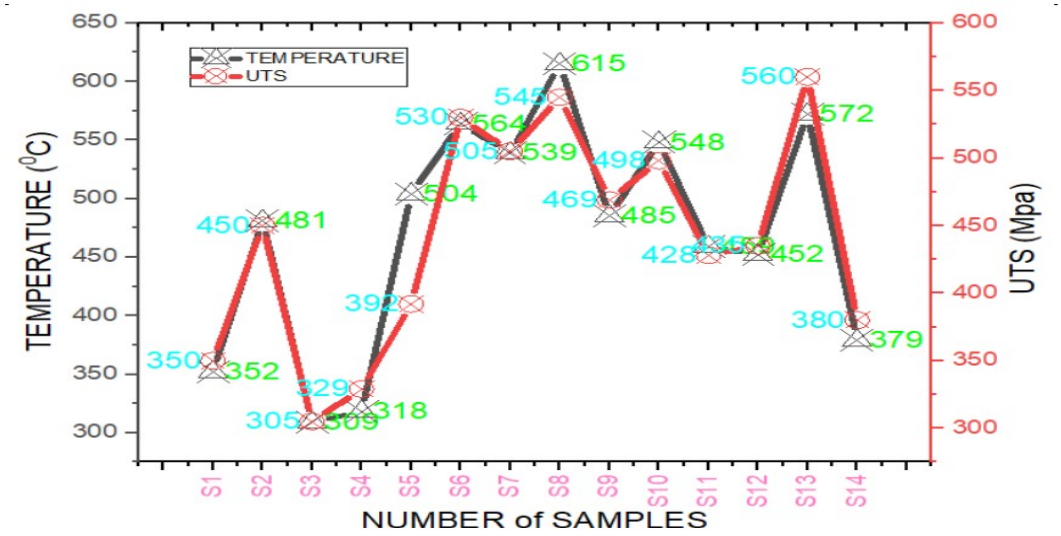

Effect of Temperature on the Hardness of the Weldment

As shown in Figure 4.9,4.10 the hardness variation of the both materials from inherent hardness value tend to increase with an increase of temperature. Relatively, the low alloy steel, AISI 4130 shows

a greater hardness variation than the austenite stainless steel, AIS304H. It is because the stainless steel is more resistant in lower temperature than the low alloy steel. However, both the materials consistent change in their hardness due to heat and showed wide amount of HAZ relatively.

Fig. 4.9: Effect temperature on the hardness of the weldment (AISI304H)

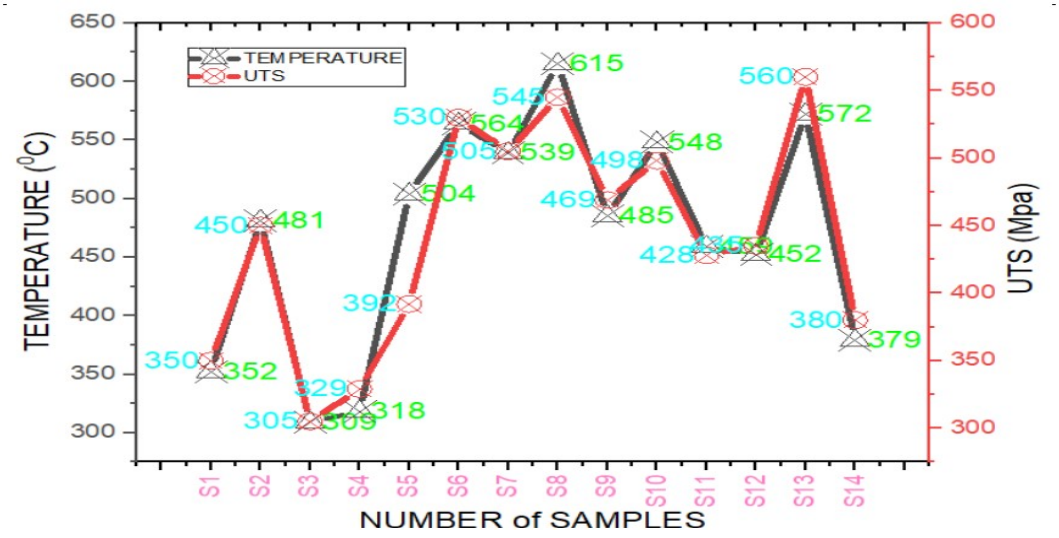

Fig. 4.10: Effect temperature on the hardness of the weldment (AISI4130)

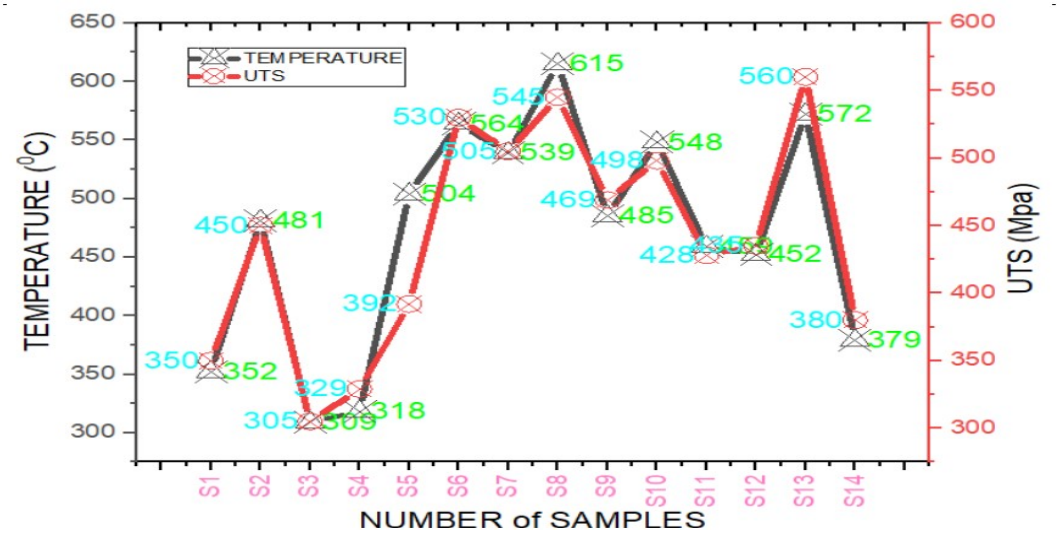

4.1.4 ***Optimization of CDFW***

Optimization of processes is caught between the growing needs for quality, high process safety, minimal manufacturing costs, and short manufacturing times. To meet the demands, manufacturing process setting parameters have to be chosen in the best possible way. The success of the manufacturing process depends upon the selection of appropriate process parameters. The selection of optimum process parameters plays a significant role to ensure the uality of the product, reducing the manufacturing cost and to increase productivity in computer-controlled manufacturing process. The first necessary step for process parameter optimization is to understand the principles governing the manufacturing process by developing an explicit mathematical model that may be mechanistic and empirical. The model in which the functional relationship between input-output and in-process parameters is determined analytically is called the mechanistic model. However, as there is a lack of

adequate and acceptable mechanistic models for manufacturing processes, the empirical models are generally used in manufacturing processes. The modeling techniques of input-output and in-process parameter relationships are mainly based on statistical regression, fuzzy set theory, and artificial neural networks.

Response Surface Methodology (RSM)

Response surface methodology (RSM) is a collection of statistical and mathematical methods that are useful for the modeling and optimization of engineering science problems. In this technique, the main objective is to optimize the responses that are influenced by various input process parameters. RSM also quantifies the relationship between the controllable input parameters and the obtained responses. In modeling and optimization of manufacturing processes using RSM, sufficient data is collected through designed experimentation. In general, a second-order regression model is developed because first-order models often give lack-of-fit. According to RSM, all the input process parameters are assumed to be measurable and the corresponding responses can be expressed as follows:

$$Y = f(X_1, X_2, \ldots., X_k) + \xi \tag{4.1}$$

Where Y is the response which is required to be optimized, f is the unknown function of response, $x_1, x_2, \ldots., x_k$ denote the independent parameters or variables, also called natural variables, k is the number of the independent variables and finally ξ is the statistical error that represents other sources of variability not accounted for by f. These sources include the effects such as the measurement error. It is generally assumed that ξ has a normal distribution with mean zero and variance.

1. Stages in RSM

   - Initial stage; the preliminary work in which the determination of the independent parameters and their levels are carried out.
   - Analysis stage; the selection of the experimental design and the prediction and verification of the model equation.
   - Decision stage; obtaining the response surface plot and contour plot of the response as a

   function of the independent parameters and determination of optimum points. It is assumed that the independent variables (input process parameters) are continuous and controllable by experiments with negligible errors. It is also required to find a suitable approximation for the true functional relationship between independent variables and responses. Usually, a second-order regression model as given below is utilized in RSM.

$$Y = b_0 + \sum_{i=0}^{n} b_i x_i + x^2 + \sum_{i=0}^{n} b_i x_2 + \sum_{i=0}^{n} b_i x_i x_j \tag{4.2}$$

2. Advantages and Draw Backs of RSM
   RSM offers a large amount of information from a small number of experiments; it is possible to observe the interaction effect of the independent parameters on the response; whereas, RSM has a difficulty of fitting the data to a second-order polynomial.

3. Selecting Factors, Their Levels and Responses

Fig. 4.11: Response surface methodology flow chart

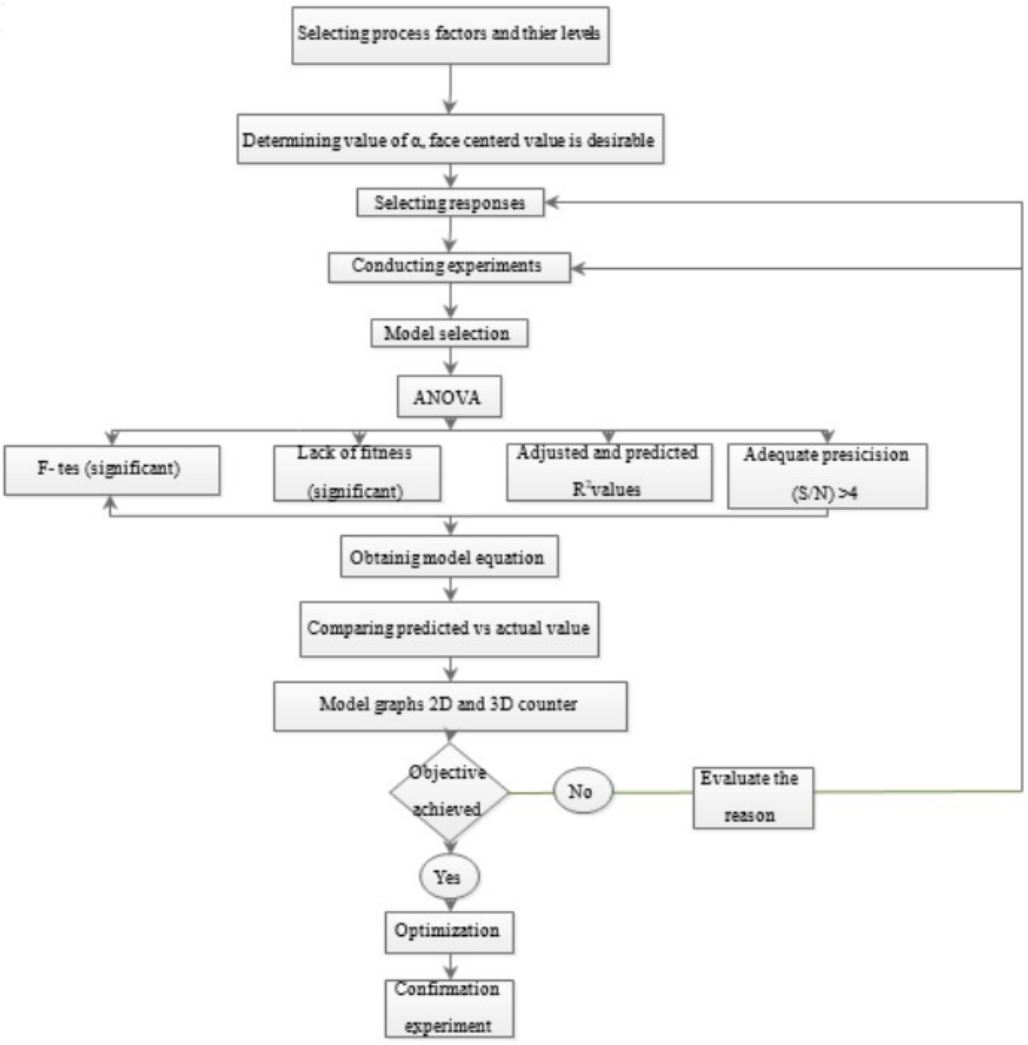

Tab. 4.4: Selected factors and levels

Factors	Number of levels			Response
	Level 1	Level 2	Level 3	
Rotational speed(rpm)	700	7900	1120	
Friction time(s)	4	7	10	UTS
Burn-off length(mm)	2	3	4	

Experimental results were conducted by the above-nominated factors and levels, thus the number of runs screened were according to response surface methodology;

Model selection

Select the highest order polynomial where the additional terms are significant and the model is not aliased. As shown in the table of fit summary; the highest order was recommended for this study due to the reason that it includes additional significant terms.

Warning: The Cubic model is aliased.

Fit Summary

Response 1: Ultimate tensile strength

Tab. 4.5: Suggested model by design expert software

Source	Sequential p-value	Lack of Fit p-value	Adjusted R^2	Predicted R^2	
Linear	< 0.0001	0.1314	0.9112	0.8557	
2FI	0.4516	0.1187	0.9109	0.6076	
Quadratic	0.0139	0.5646	0.9864	0.9336	Suggested
Cubic	0.5646		0.9846		Aliased

Tab. 4.6: Suggested lack of fit b DOE

Source	Sum of Squares	DF	Mean Square	F-value	p-value	
Mean vs Total	2.724^{06}	1	2.724^{06}			
Linear vs Mean	80832.00	3	26944.00	45.48	< 0.0001	
2FI vs Linear	1762.60	3	587.53	0.9884	0.4516	
Quadratic vs 2FI	3798.00	3	1266.00	13.95	0.0139	Suggested
Cubic vs Quadratic	158.12	2	79.06	0.7713	0.5646	Aliased
Residual	205.00	2	102.50			
Total	2.811^{06}	14	2.008^{05}			

Lack of Fit Tests

Tab. 4.7: Summary of the suggested model

Source	Std. Dev.	R^2	Adjusted R^2	Predicted R^2	PRESS	
Linear	24.34	0.9317	0.9112	0.8557	12520.64	
2FI	24.38	0.9520	0.9109	0.6076	34039.60	
Quadratic	9.53	0.9958	0.9864	0.9336	5764.18	Suggested
Cubic	10.12	0.9976	0.9846			Aliased

Focus on the model maximizing the Adjusted $R^2$and the Predicted R^2 is critical.

ANOVA for Quadratic Model

Analysis of variance is a standard statistical technique to interpret the experimental results. It's extensively used to detect differences in the average performance of groups of items under investigation. It breaks down the variation within the experimental result into various sources and so realizes the parameters whose contribution to the total variation is critical. So the analysis of variance was employed to review the relative influences of multiple variables and their significance.
Response 1: Ultimate tensile strength

Tab. 4.8: ANOVA for quadratic model

Source	Sum of Squares	DF	Mean	Square F-value	p-value	
Model	86392.60	9	9599.18	105.74	0.0002	significant
A-RS	52551.46	1	52551.46	578.89	< 0.0001	
B-FT	1128.76	1	1128.76	12.43	0.0243	
C-BL	2385.58	1	2385.58	26.28	0.0069	
AB	118.71	1	118.71	1.31	0.3166	
AC	212.34	1	212.34	2.34	0.2009	
BC	955.70	1	955.70	10.53	0.0315	
A^2	62.90	1	62.90	0.6928	0.4520	
B^2	2576.21	1	2576.21	28.38	0.0060	
C^2	1761.51	1	1761.51	19.40	0.0116	
Residual	363.12	4	90.78			
Lack of Fit	158.12	2	79.06	0.7713	0.5646	not-significant
Pure Error	205.00	2	102.50			
Cor Total	86755.71	13				

Sum of squares: the sum of the square-off deviations of the fitted response values from the mean response value, it was a measure of deviation for different components of the model. The total DF was the quantity of information in the statistics. The analysis uses that information to estimate the values of unknown population parameters. Mean squares: measure how much variation a term or a model explains. Factor coding is coded.

Sum of squares is Type III - Partial

The Model F-value of 105.74 implies the model is significant. There is only a 0.02% chance that an F-value this large could occur due to noise.

P-values less than 0.0500 indicate model terms are significant. In this case, a, B, C, BC, B^2, C^2 are significant model terms. Values greater than 0.1000 indicate the model terms are not significant. If there are many insignificant model terms (not counting those required to support hierarchy), model reduction may improve your model.

The Lack of Fit F-value of 0.77 implies the Lack of Fit is not significant relative to the pure error. There is a 56.46% chance that a Lack of Fit F-value this large could occur due to noise.

Non-significant lack of fit is good – the model is needed to fit.

Fit Statistics

Tab. 4.9: Fit statistics of R^2

Std. Dev.	9.53	R^2	0.9958
Mean	441.14	Adjusted R^2	0.9864
C.V. %	2.16	Predicted R^2	0.9336
	Adeq Precision		31.5713

The Predicted R^2 of 0.9336 is in reasonable agreement with the Adjusted R^2 of 0.9864; i.e. the difference is less than 0.2.

Adeq Precision measures the signal to noise ratio. A ratio greater than 4 is desirable. Your ratio of 31.571 indicates an adequate signal. This model can be used to navigate the design space.

Coefficients in Terms of Coded Factors

Tab. 4.10: Coefficients in terms of coded factors

Factor	Coefficient Estimate	df	Standard Error	95% CI Low	95% CI High	VIF
Intercept	474.63	1	6.77	455.82	493.44	
A-RS	85.97	1	3.57	76.05	95.89	1.26
B-FT	12.12	1	3.44	2.58	21.66	1.09
C-BL	17.11	1	3.34	7.84	26.37	1.23
AB	-5.09	1	4.45	-17.45	7.27	1.31
AC	-5.92	1	3.87	-16.67	4.83	1.15
BC	14.40	1	4.44	2.08	26.72	1.30
A^2	4.74	1	5.69	-11.06	20.54	1.14
B^2	-29.77	1	5.59	-45.29	-14.26	1.11
C^2	-26.68	1	6.06	-43.50	-9.86	1.15

The coefficient estimate: represents the expected change in response per unit change in factor's value when all remaining factors are held constant. The intercept in an orthogonal design is the overall average response of all the runs. The coefficients are adjustments around that average based on the factor settings. When the factors are orthogonal the VIFs are 1; VIFs greater than 1 indicate multi-collinearity, the higher the VIF the more severe the correlation of factors. As a rough rule, VIFs less than 10 are tolerable.

Confidence intervals (CI): ranges of values that are possible to enclose the exact value of the coefficient for all terms in the model.

Final Equation in Terms of Coded Factors

$$Y = f(RS, FT, BL) \tag{4.3}$$

$$UTS = 474.63+85.97A+12.12B+17.11C-5.09AB-5.92AC+14.40BC+4.74A^2-29.77*B^2-26.68*C^2 \tag{4.4}$$

The equation in terms of coded factors can be used to make predictions about the response for given levels of each factor. By default, the high levels of the factors are coded as +1 and the low levels are coded as -1. The coded equation is useful for identifying the relative impact of the factors by comparing the factor coefficients.

Final Equation in Terms of Actual Factors

$$Y = f(RS, FT, BL) \tag{4.5}$$

$$UTS = -318.41433+0.355005RS+43.30713FT+169.25446BL-0.008081RSFT-4.79976RS*BL+4.79976F$$ (4.6)

The equation in terms of actual factors can be used to make predictions about the response for given levels of each factor. Here, the levels should be specified in the original units for each factor. This equation should not be used to determine the relative impact of each factor because the coefficients are scaled to accommodate the units of each factor and the intercept is not at the center of the design space.

Predicted vs Actual

Actual vs. Predicted: A graph of the predicted response values versus the actual experimental response values. The objective was to identify value, or collection of values, that were not simply **predicted by the model. R-squared**: A measure of the amount of variation around the mean explained by the model. R^2 =0.9336% which means 6.64% variation which was acceptable.

Fig. 4.12: Predicted vs Actual graph

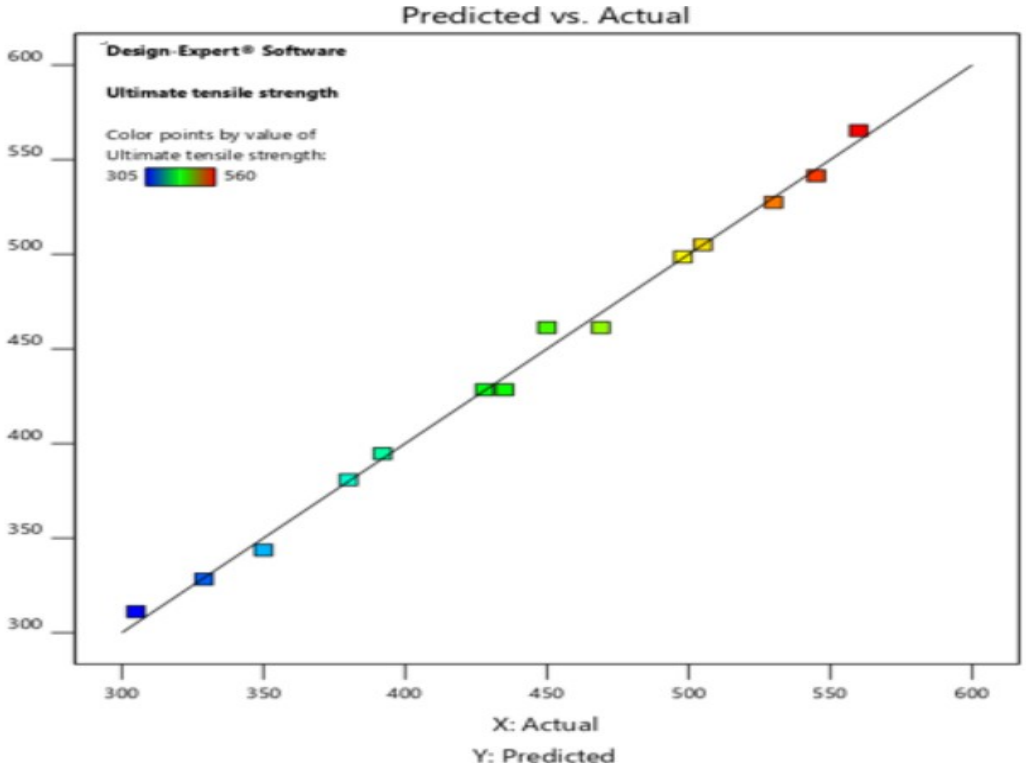

Tab. 4.11: Errors encountered between experimental and predicted results

Number of runs	Factors Experimental			result(Mpa)	Predicted results (Mpa)	% error
	Rotational	speed Friction time	Bur off length			
1	700	7	2	350	343.335	1.94
2	900	7	4	450	461.253	-2.44
3	700	4	2	305	311.108	-1.96
4	700	4	4	329	328,361	0.19
5	900	10	2	392	394.668	-0.68
6	1120	7	2	530	527.467	0.48
7	1120	4	2	505	505.65	-0.12
8	1120	10	4	545	541.494	0.65
9	900	7	4	469	461.253	1.68
10	1120	4	4	498	498.639	-0.13
11	900	4	3	428	428.413	-0.096
12	900	4	3	435	428.413	-0.94
13	1120	7	3	560	565.33	-0.94
14	700	10	3	380	380.838	-0.22

$$\% \text{ error} = \frac{Experimentalvalue - predictedvalue}{predictedvalue}$$

Residual vs predicted

Residuals vs. Predicted: The plot of the errors versus the ascending predicted/expected response values. It investigates the assumption of continuous alteration with a random scatter.

Fig. 4.13: Residual vs predicted graph

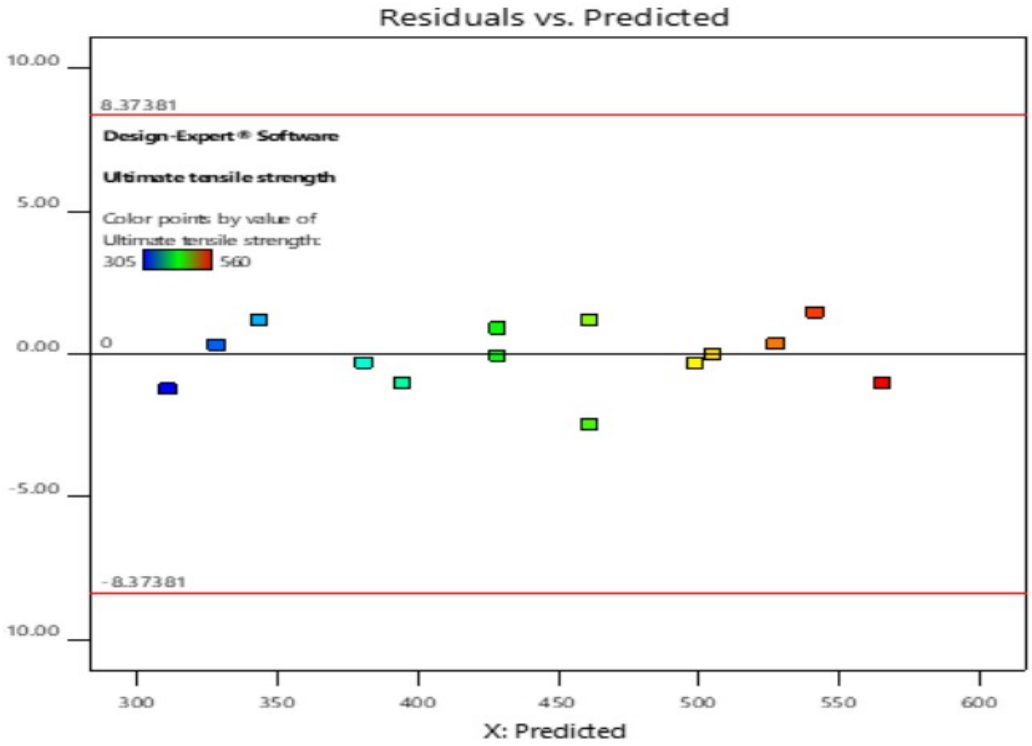

Residual vs Run

Residuals vs. Run order: This graph was a plot of the errors versus the run order of the experiment. It displays the prowling variables that may have effects on the response values during the experimentation.

Fig. 4.14: Residual vs run graph

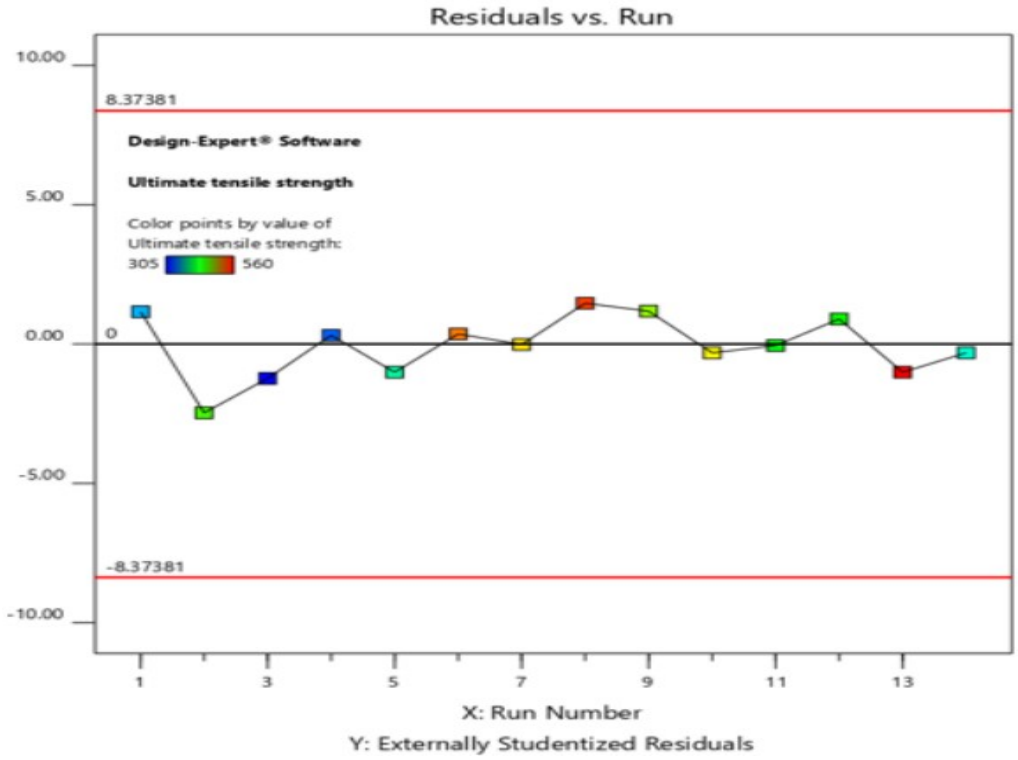

Box-cox plot for power transformation

Box-Cox Plot for Power Transforms: The plot offers instruction for choosing the exact power law transformation. The suggested transformation for the current model was none, depending on the best lambda value, which originated at the bottom point of the curve produced by the natural log of the sum of squares of the residuals. The best lambda and current lambda were 2.37, and the current lambda is in the 95% confidence interval (-0.03, 4.50).

Fig. 4.15: Box-cox plot for or transformation

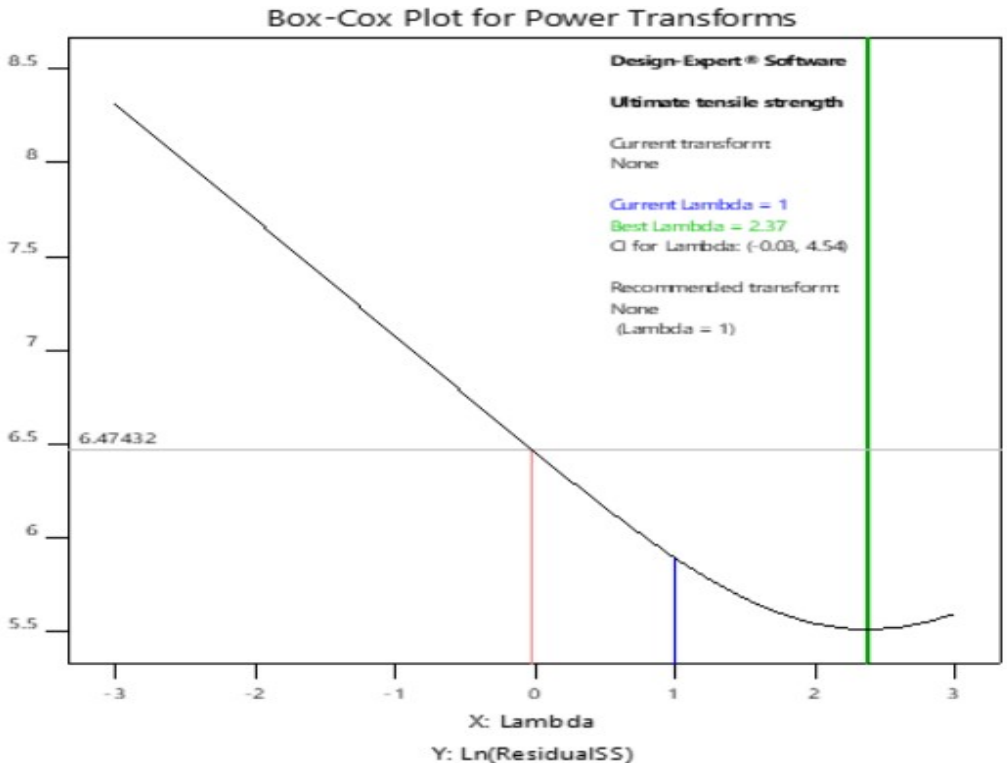

Cooke's distance

The table below contains descriptions of each case statistic. The values in this report table were used to produce the diagnostics graphs. Actual Value: The recorded experimental data of the response for each experiment. Predicted Value: The predicted values from the model were generated using the prediction equation and includes block and center-point corrections when they were part of the design experiment. Residual: The change between experimentally recorded data and the Predicted values for each experiment number. Leverage: Leverage of a point differs from zero to unity and it shows how much a single design point which affects the model's predicted values. A leverage of 1 indicates the predicted value at that specific case would accurately equal the experimental recorded value of the process, i.e., the error will be zero. The summation of leverage values across all cases equals the number of coefficients (containing the constant) fit by the model. The extreme leverage an experimental can have is $\frac{1}{k}$, where k is the number of times the experimentation is replicated. Cook's Distance: A degree of how much the regression could variation if the situation was absent from the examination. Comparatively large values are related to circumstances with high leverage and large studentized errors. Cases with large Di values comparative to the other cases should be examined they could be produced by recording residuals, an improper model, or a design point far from the remaining cases.

Fig. 4.16: Cook's Distance graph

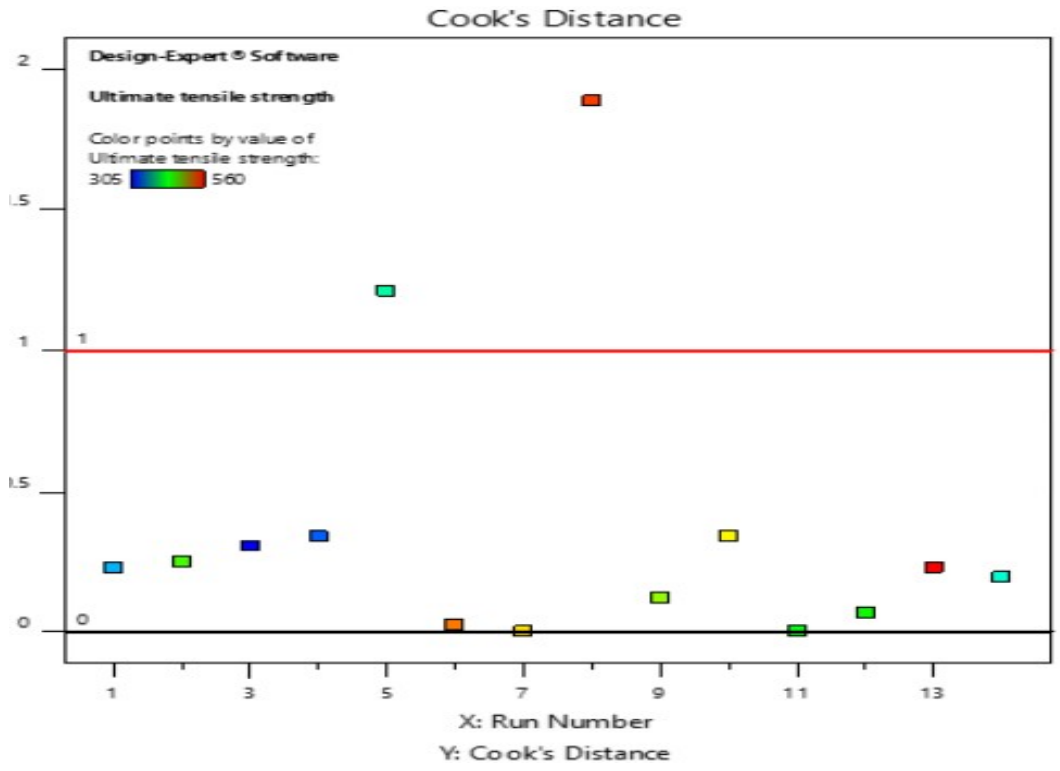

Tab. 4.12: Diagnostics report

Run Order	Actual Value	Predicted Value	Residual	Leverage	Internally Studentized Residuals	Externally Studentized	DFFITS Cook's Distance	Influence on Fitted Value	Standard Order
1	350.0	343.7	6.31	0.65	1.113	1.160	0.226	1.567	3
2	450.0	461.3	-11.25	0.480	-1.637	-2.469	0.247	-2.371	12
3	305.0	311.1	-6.11	0.695	-1.161	-1.234	0.307	-1.863	1
4	329.0	328.4	0.6388	0.964	0.355	0.313	0.342	1.627	10
5	392.0	394.7	-2.67	0.923	-1.007	-1.010	1.211(1)	-3.489(1)	5
6	530.0	527.5	2.53	0.575	0.408	0.361	0.022	0.419	4
7	505.0	505.1	-0.065	0.853	-0.018	-0.015	0.000	-0.037	2
8	545.0	541.5	3.51	0.919	1.291	1.464	1.886(1)	4.926(1)	14
9	469.1	461.3	7.75	0.480	1.127	1.182	0.117	1.135	13
10	498.0	498.6	-0.639	0.964	-0.355	-0.313	0.342	-1.627	11
11	428.0	428.4	-0.413	0.436	-0.058	-0.050	0.000	-0.044	6
12	435.0	428.4	6.59	0.436	0.921	0.898	0.066	0.790	7
13	560.0	565.3	-5.34	0.691	-1.007	-1.010	0.227	-1.509	8
14	380.0	380.8	-0.838	0.939	-0.355	-0.313	0.193	-1.223	9

4.1.5 ***Interactions***

Interaction between friction time and UTS

Fig. 4.17: Interaction between burn off length and UTS

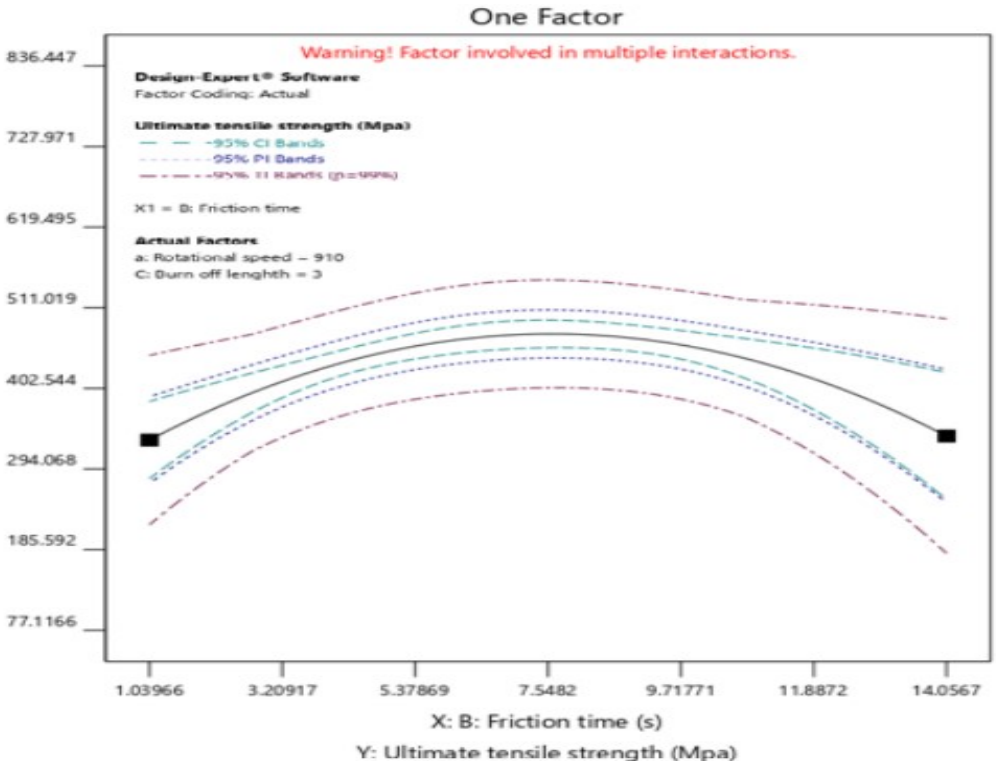

Fig. 4.18: Interaction between burn off length and UTS

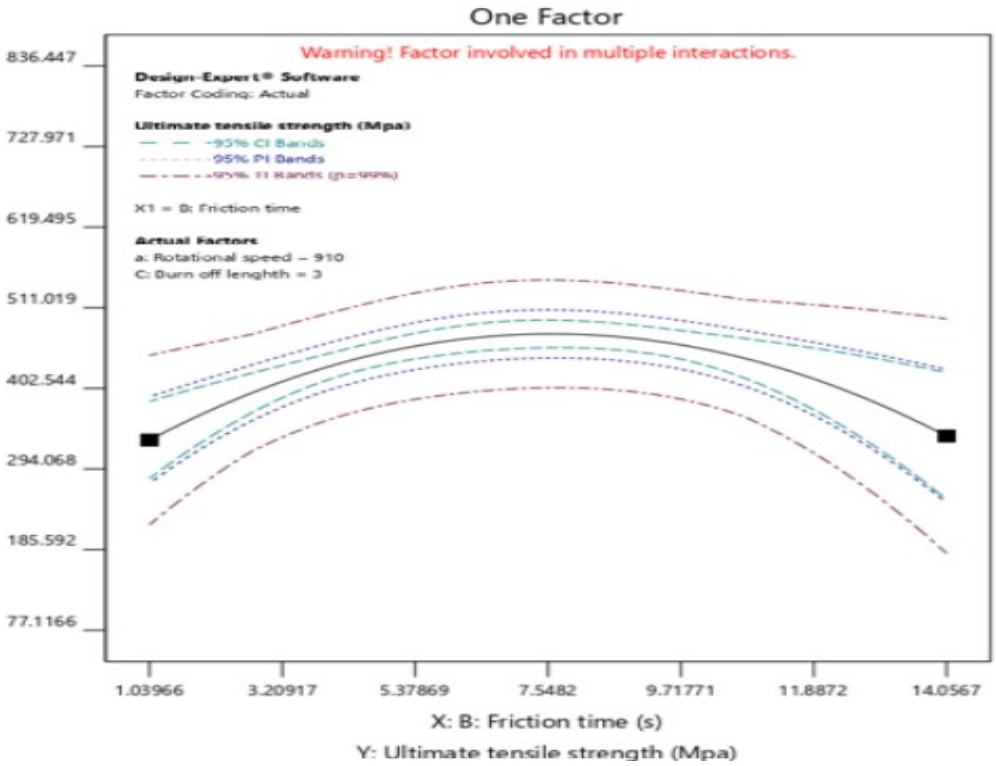

Fig. 4.19: Interaction between rotational and UTS

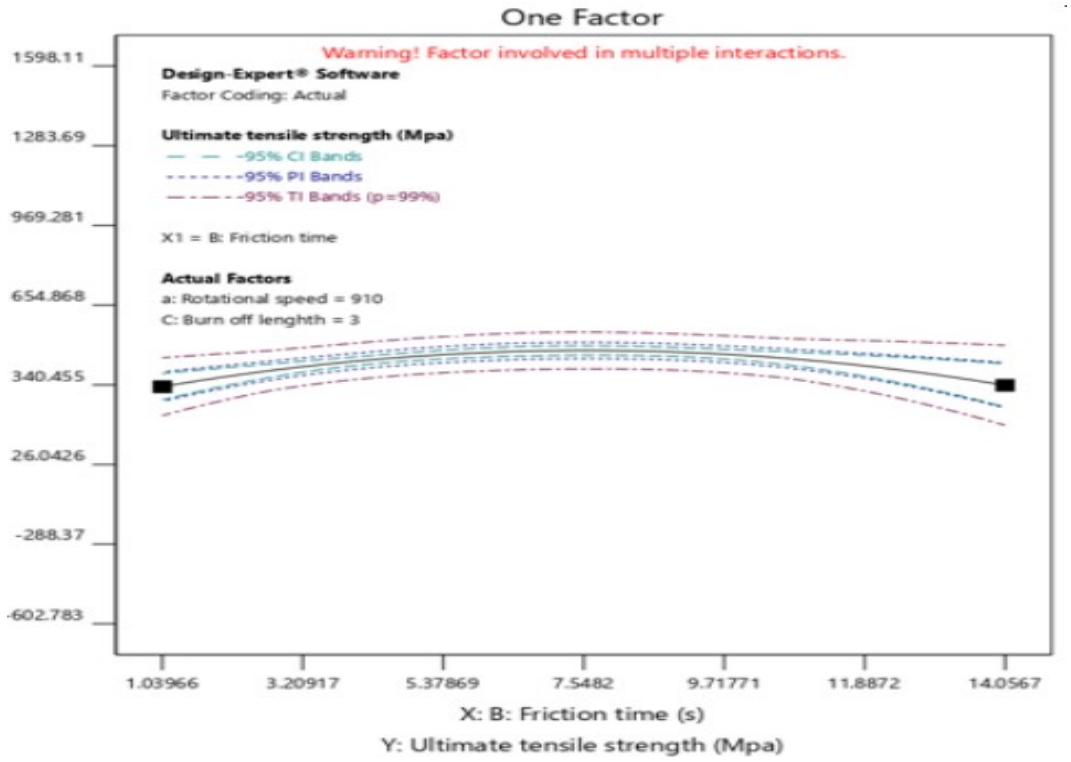

4.1.6 Optimization results

The optimization section examines a combination of factor levels that simultaneously fulfill the conditions located on each of the responses and factors/parameters. To comprise a response in the optimization conditions it must have a model that is suitable through investigation or provided via an equation. The likely goals were: maximize, minimize, target, within range, none (for responses only) and set to an exact value (parameters only.) In this work, the goals were to maximize for response and in range for all factors. Graphical optimization uses the models to show the volume where acceptable response outcomes could be found. The summary table below shows all of the criteria applied to find the optimal settings.

Report

Constraints: the following constraints were been taken in optimizing the experimental results

Tab. 4.13: Constraints criteria for optimization

Name	Goal	Lower Limit	Upper Limit	Lower Weight	Upper Weight	Importance
A:Rotational speed	is in range	700	1120	1	1	3
B:Friction time	is in range	4	10	1	1	3
C:Burn-off length	is in range	2	4	1	1	3
UTS	maximize	305	560	1	1	3
StdErr(UTS)	minimize	6.2919	9.35661	1	1	3

Post analysis

(II) **Factors**

Tab. 4.14: Predicted levels of all factors

Factor	Name	Level	Low Level	High Level	Std. Dev	Coding
A	Rotational speed	1101.19	700.00	1120.00	0.0000	Actual
B	Friction time	7.99	4.00	10.00	0.0000	Actual
C	Burn-off length	3.73	2.00	4.00	0.0000	Actual

(II) **Confirmation location**

Tab. 4.15: Confirmed results

Rotational speed	Friction time	Burn off length
1101.26	8.00141	3.7351

(III) **Ramps**

Fig. 4.20: Optimized results in terms of ramps

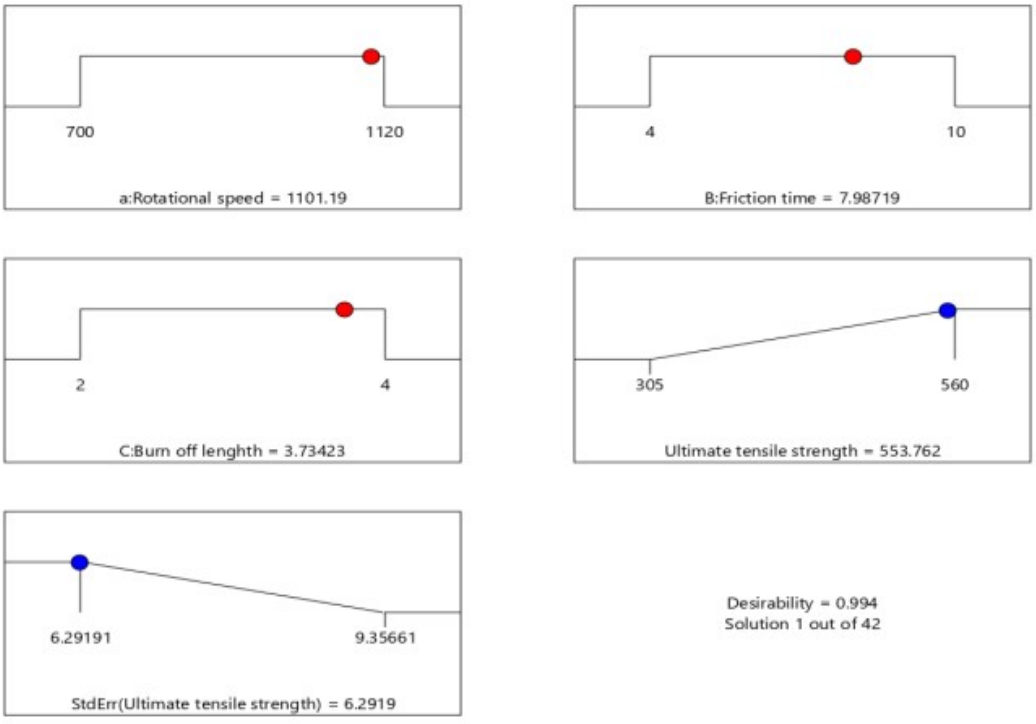

(IV) **Desirability**

Fig. 4.21: Desirability graph

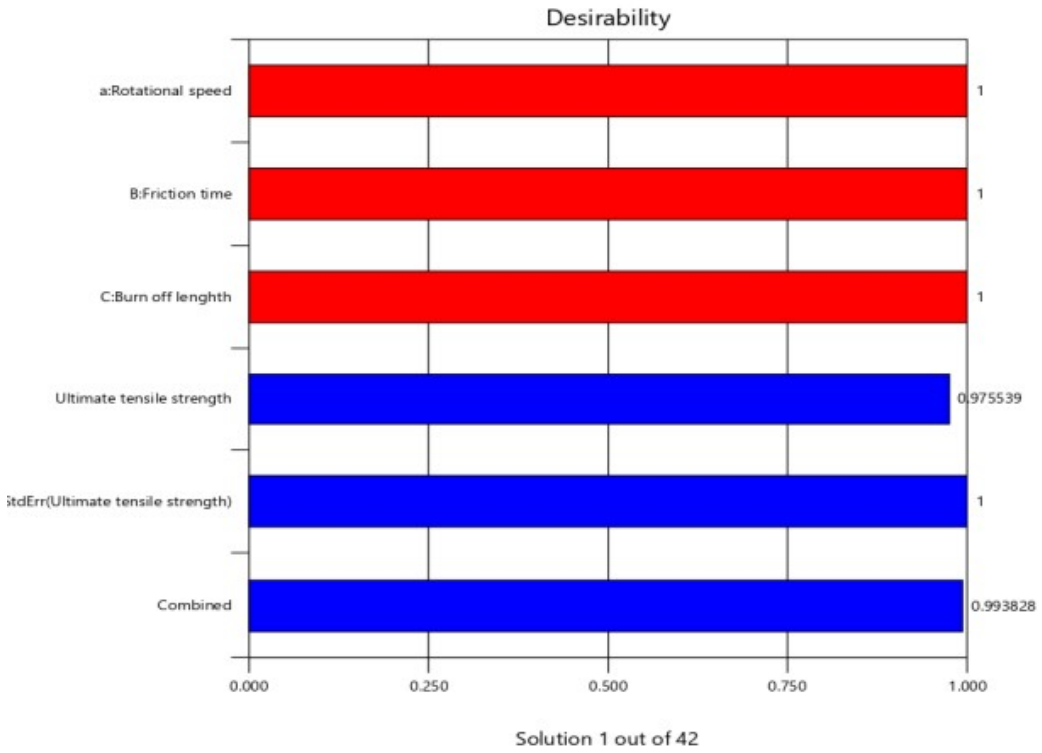

(V) **Confirmation** Two-sided Confidence = 95%

Tab. 4.16: Two side confidence confirmation

Soolution 1 of 42 Response	Predicted Mean	Predicted Median	observed	Std Dev	dof	SE predicted	95% PI low	Data Mean	95% P
UTS	553.8	553.8		9.5	1	11.4	522.0		585.4

Table 4.16, shows predictions at the levels of the selected factors along with error estimates used to compute statistical intervals. SE Mean: the standard error of the mean was the measure of the dispersion of means around the total mean. Tolerance interval: is an arithmetic interval within which, with some confidence level, a quantified amount of sampled falls. The table compares the prediction interval of the model to a follow-up sample's average. Since the average was in the prediction interval (522.062<553.762<585.464) the model was confirmed.

4.1.7 ***Discussion***

As per the results found from lab, experiment and from the software (design of expert); the results have shown that; the dissimilar steel bars which were welded on a direct drive set up lathe machine showed a reasonable welding quality and the fracture was found in the weakest part of the parent material. Hence the welding strength of the weldment exceeds the inherent strength of AISI 304H.The hardness and temperature results conducted are in reasonable agreement with tensile strength of the lab results.

Fig. 4.22: Comparison between weldment strength and inherent parent material strength

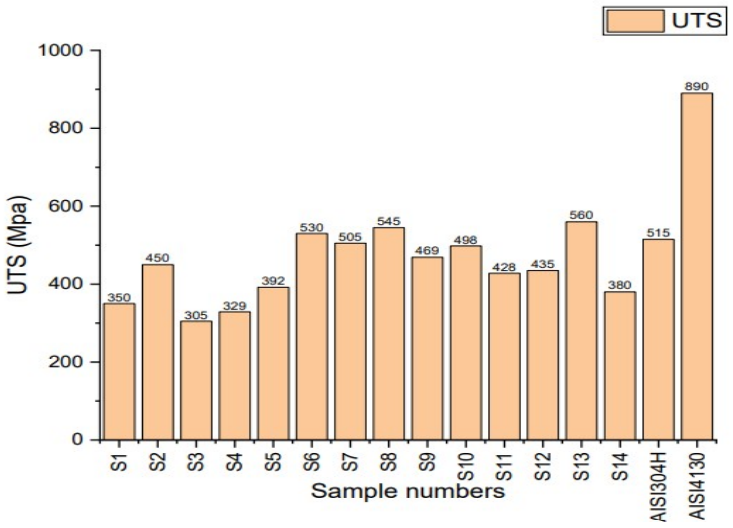

An optimization result of the current study in Table 4.17,is being compared with related studies of few researchers. Hence the current study showed reasonable agreement with the results of prior results.

Tab. 4.17: Comparison studies with the current study

Findings	Current study	[33]	[13]	[9]
Material/s joined	AISI 304H and AISI 4130	AISI 1020-ASTM A536 joints	Steel with variation C	AISI 304 with AISI 1021
UTS(Mpa)	560	496	7,889 Kg/cm2	472
Friction machine	CDFW universal lathe machine	CDFW machine type of ZT-13	HMT LB-17 lathe machine	conventional heavy duty lathe machine
Factors and levels	3*3	3*3	3*2	2*2
Max-Hardness	Interface	Interface	Interface	interface Interface

In addition as shown in illustrates an increase of hardness in the interface of the welded material relative to their combination of factors and it compared with the dissimilar steel bars inherent hardness values.

Fig. 4.23: Comparison between interface hardness and inherent parent material hardness

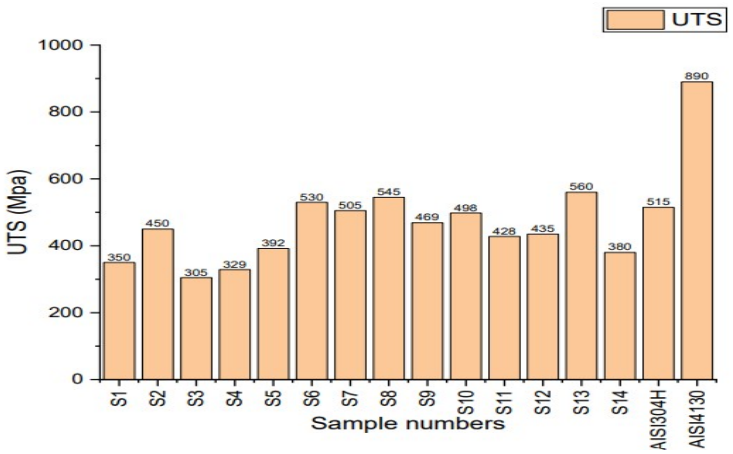

An optimization results are also discussed in the forgoing table as shown in the Table A.2

Tab. 4.18: Comparison between interface hardness and inherent parent material

Criteria	Current study	[33]	[13]
Selected model	Quadratic	Quadratic	Linear
Lack of fit	Not significant	Not significant	Significant
Coefficient R^2	0.9958	0.97	0.682151
Adjusted R^2	0.9864	0.95	0.622554
Predicted R^2	0.9336	0.74	0.477034
Adeq Precision	31.5713	24.23	12.65784
%error of predicted vs actual	MAX=2.44 Max=2.35	Min=0.096 Min=1.75	

4.1.8 2D and 3D Graph Counters

Ultimate Tensile Strength

Fig. 4.24: 2D and 3D graphs of ultimate tensile strength (rotational speed vs burn-off length)

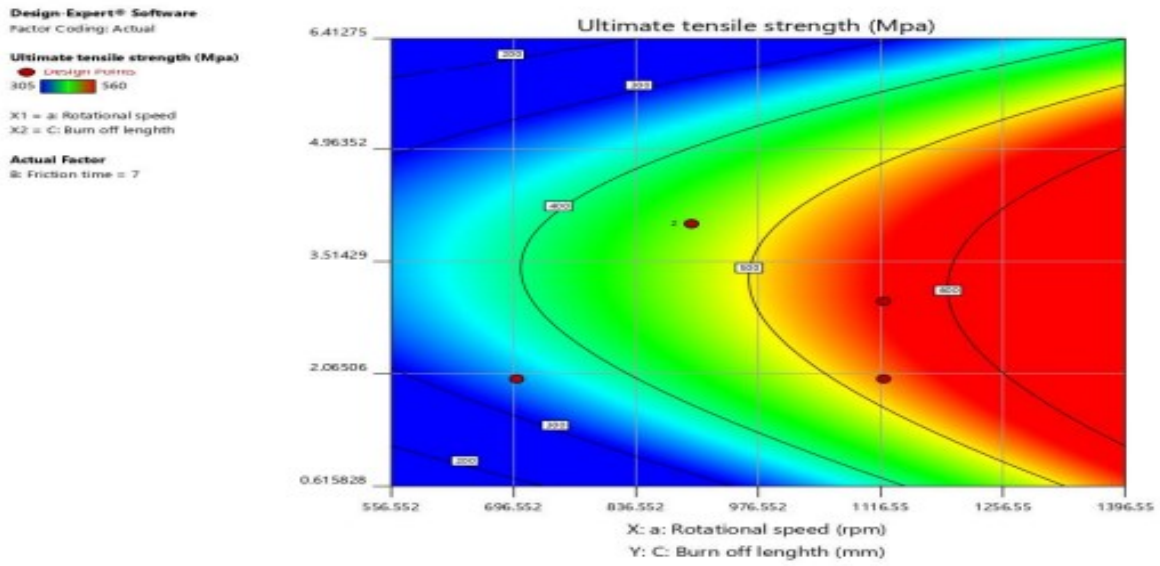

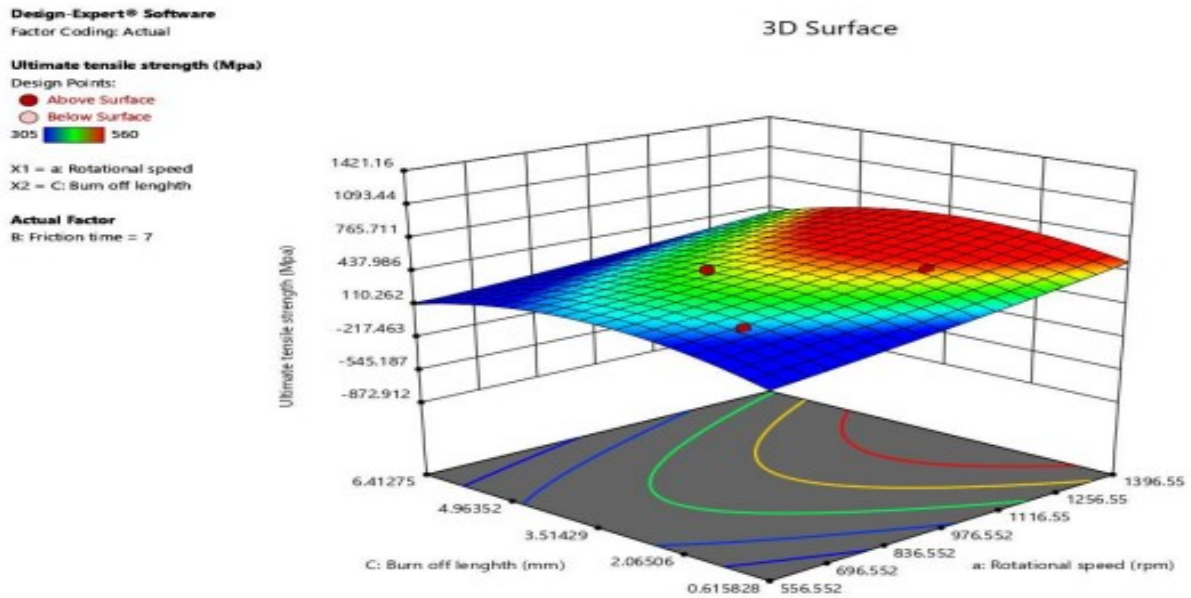

Fig. 4.25: 2D and 3D graphs of ultimate tensile strength (Friction time vs Burn-off length

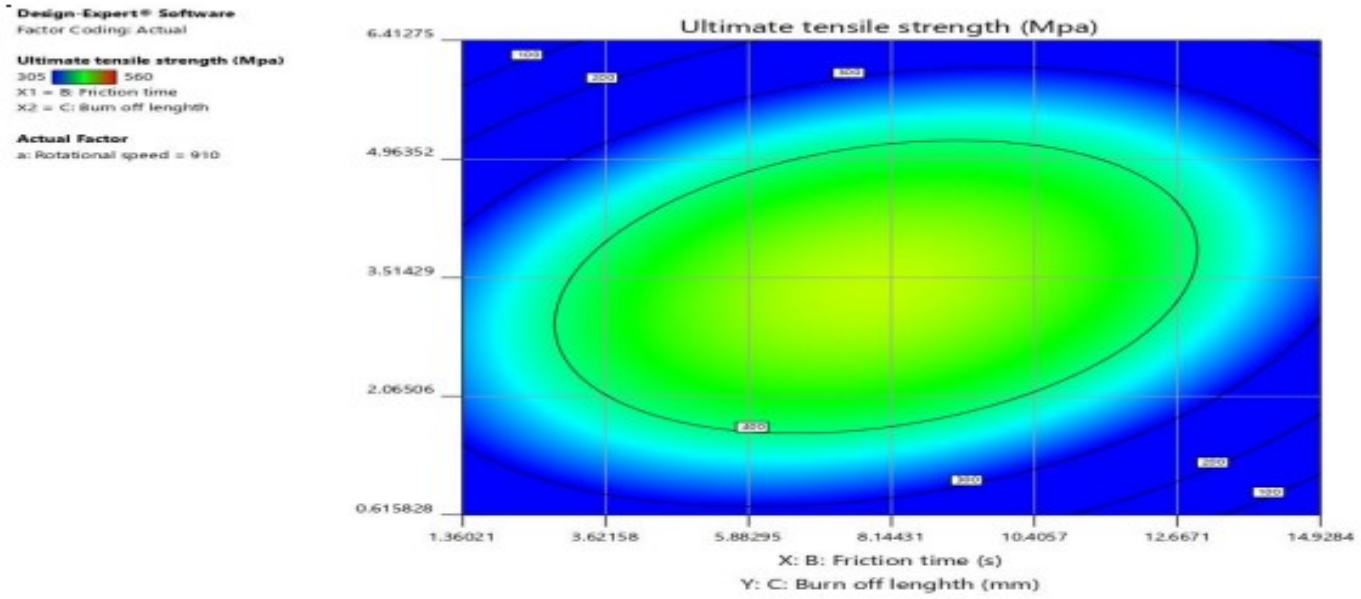

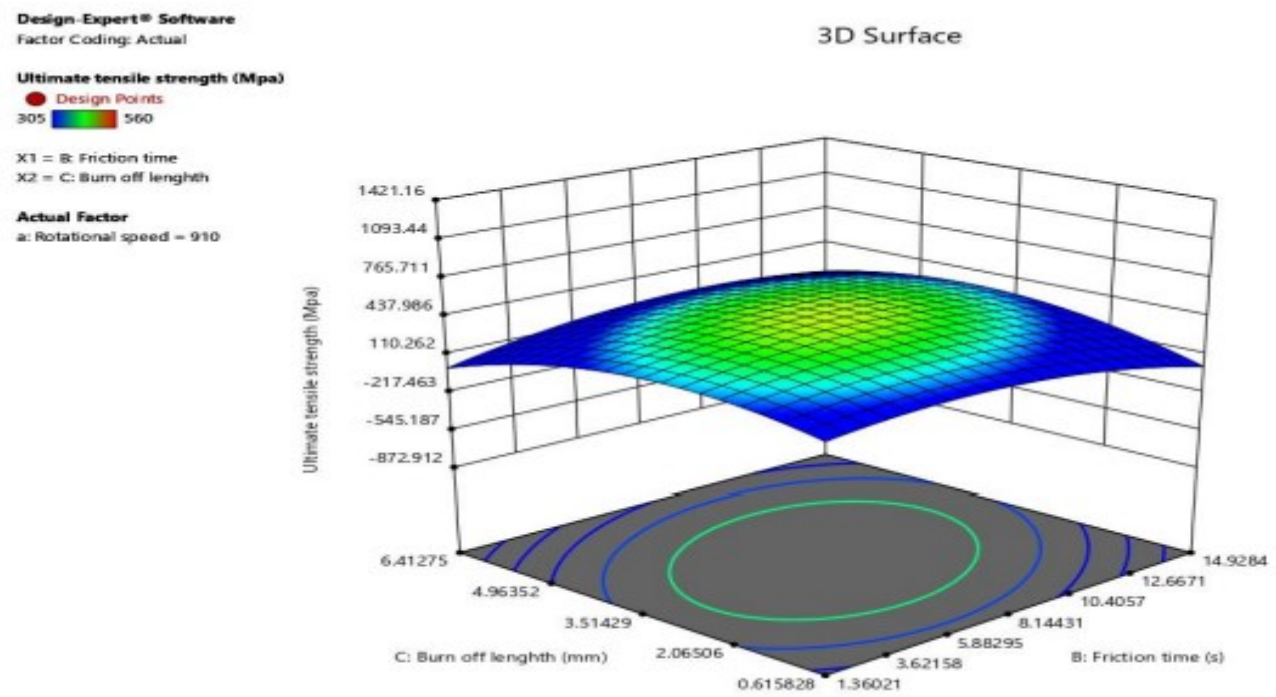

Fig. 4.26: 2D and 3D graphs of ultimate tensile strength (Friction time vs Rotational speed)

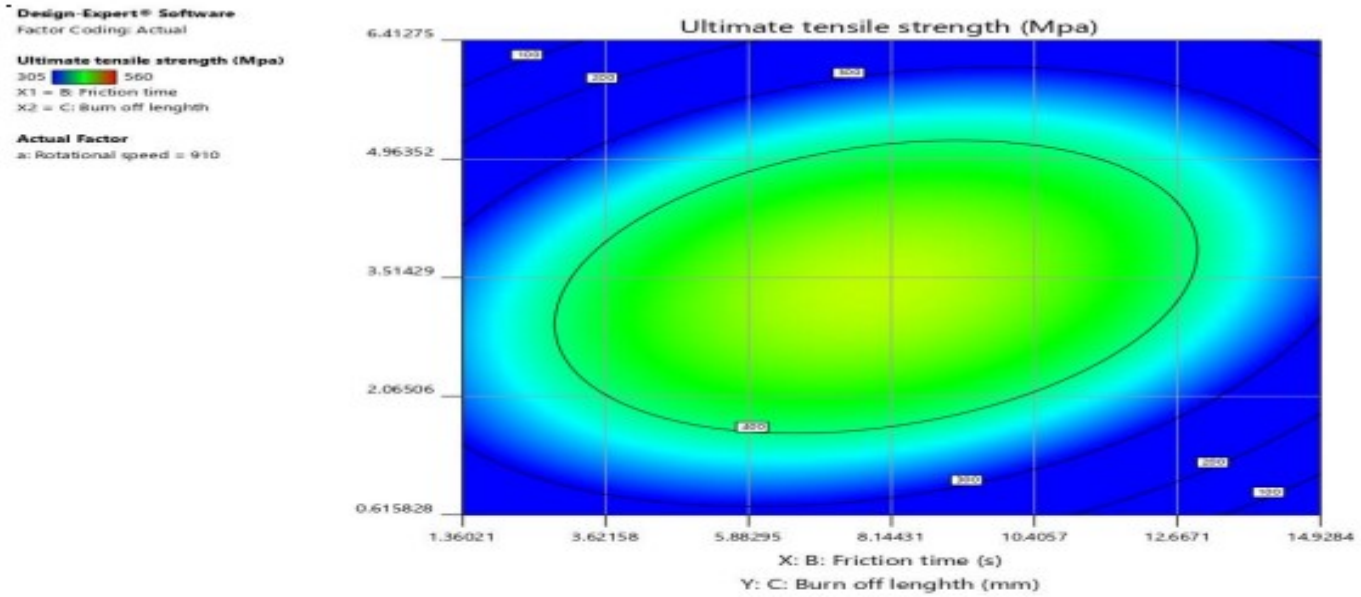

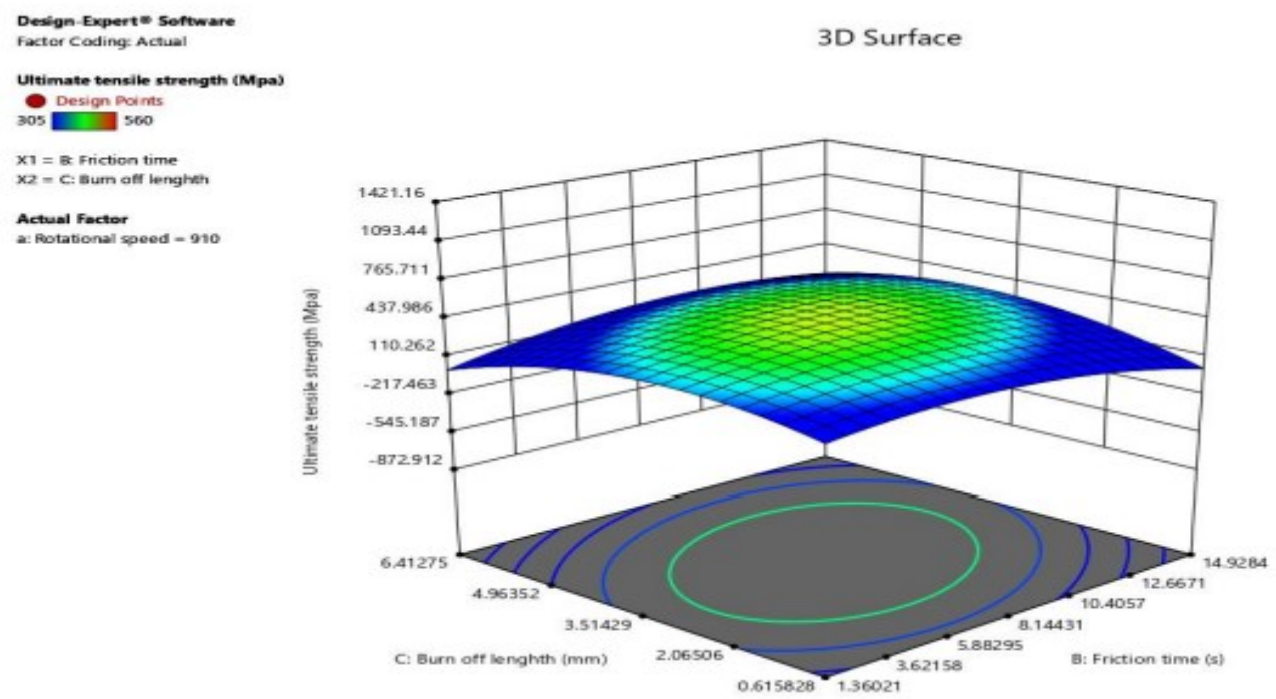

5

CONCLUSION and RECOMMENDATION

5.1 ***Conclusions***

According to the results concluded and discussed in the forgoing topics the following conclusions are drawn;

1. **Tensile strength**

   - Continuous drive friction welding machine was found to be successful for the production of AISI 304H–AISI 4130 steel weldment.
   - The laboratory built friction welding set-up was found to be successful for the production of friction welds
   - The rotational speed of the process has been found to be an influential parameter for the friction welding process; hence strength of the weldment have steadily increased with an increase of rotational speed
   - The maximum tensile strength of the weldment was obtained at 1200 Rpm at sample 13(see the other combination in the figure below).
   - The tensile strength of the weldment tends to decrease as the friction time increased beyond and blow 7s.
   - Lack of proper interlocking was observed when the friction time was 4s, due to the lack of heat created in the interface during friction welding.
   - High amount of burn-off length have created poor welding quality by creating high HAZ, hence minimizes the quality of the welds.
   - Less amount of burn-off length has created lesser welding quality; decreasing burn-of length creates improper interlocking between the welds and weakens the bond.

2. **Micro hardness**

   - Hardness of the weldment is higher in the interface of the welded parts.
   - The highest hardness value achieved was 33 HRC(see figure above)
   - Increases of hardness were shown in samples having greater burn-off length.

- Increased friction time has also an influential role in creating high hardness especially when it was accompanied with higher amount of burn-off length and rotational speed.
- Lesser strength of weldment was exhibited in samples which possesses higher Hardness.

3. **Optimization**

- Quadratic model is the suggested model for the experimental results.
- Experimentally conducted values and software predicted value tend to resemble very smooth.
- The lack of fit is not significant relative to the pure error and there was a 56.46lack of fit could occur due to noise.
- Most of the errors encountered in this experiment was due noise (error in measurement and instrumentation).
- No transformation was recommended in the suggested model.

*5.2 **Recommendations***

On the way of working the current study; there have been a couple of stumble blocks hinders the study not to reach at its best time. Those were;

- Willingness of cooperation from enterprises to help students to carry out their thesis.
- Lack of test instruments in universities and industries.
- Lack availability materials in market.

While conducting the current study experimentation, Jimma University had one lathe machine in order, it was suggested that there had been a phenomenon in friction welding which led to a disorder of the lathe machine. And an advice was given not to take the risk, thus it was indispensable to seek another machines to work with, most of the small enterprise owners were reluctant to give it a try. Hence it is recommendable that;

- Universities should arrange a working ground for their students or create a strong link with industries in hand.
- Students should bring their best conduct to the industries.

Specifically to the research area, anyone who is having willingness in studying rotary friction welding is recommended to address the following issues;

- Availability of raw materials should be put in mind.
- Chemical composition test should be prior to the experimentation.
- Prior preparation activities for experimentation such as cleaning, cutting, and etching should be carried out cautiously.
- Prior preparation of samples for experimentation according to standards is vital.
- Prior preparation of samples for lab tests according to accepted standards is also vital.

5.2.1 ***Future Works***

Obviously Continuous Drive Friction Welding (CDFW) constitutes various working parameters (see figure 4). Three parameters are studied thoroughly in the current study and other parameters can be used to study CDFW as well. Thus, the following future works can be studied in this very study.

- As the current study was carried out using material with same diametrical dimension; thus; to study with materials having different diametrical dimension is advisable.
- Material surfaces which were exposed to frictional contact were having plain surface; thus using different configuration surface such as tapered can be used to create better interlocking between interfaces; hence create better welding joint.
- Rate of temperature can be studied by using contact temperature device.
- Different cooling media can be used to study their effects on weld quality.

Bibliography

[1] Akata, H. E. (2009). An investigation on the effect of dimensional differences in friction welding of AISI 1040 specimens. Industrial Lubrication and Tribology, 55, 223 -232 https://doi.org/10.1108/00368790310488887

[2] Alvise, L. D., Massoni, E., and Walløe, S. J. (2002). Finite element modelling of the inertia friction welding process between dissimilar materials. 126, 387–391.

[3] Cheepu, M., and Che, W. S. (2019). Effect of Burn-off Length on the Properties of Friction Welded Dissimilar Steel Bars. 12–21.

[4] Ates, H.,and Kaya, N. (2013). Effect of Friction Time on Microstructure and Mechanical Properties of Friction Welded AISI 304 Stainless Steel to AISI 1060 Steel. Institute of Science and Technology, 06500 Ankara, Turkey, 35(2),241–252.

[5] Ates, H., and Kaya, N. (2014). Mechanical and microstructural properties of friction welded AISI 304 stainless steel to AISI 1060 steel. Princeton University Library.59(3) https://doi.org/10.2478/amm-2014-0142

[6] Dawood, B.A, Butt, I.S., hussain, G., Siddiqqi, A.M., and Zhang, F. (2017). Thermal Model of Rotary Friction Welding for Similar and Dissimilar Metals. https://doi.org/10.3390/met7060224

[7] Deulkar, S. S., Sidhu,J. S., and Lathkar , G. S. (2016). Experimental and Numerical Analysis of the Friction Welding Process for the 4340 Steel and Mild Steel Combinations. 87(July).Retrived from http://inpressco.com/category/ijce

[8] Groover, M. P. (2010). Fundamentals of modern manufacturing: materials, processes and systems. United States of America: John, W and Sons, INC. Retrieved from http://www.wiley.com/go/returnlabel

[9] Handa, A., and Chawla, V. (2013). Experimental study of mechanical properties of friction welded AISI 1021 steels. 38, 1407–1419.

[10] Handa, A., and Chawla, V. (2014). Experimental evaluation of mechanical properties of friction welded AISI steels. Cogent Engineering, 30(1), 1–10. https://doi.org/10.1080/23311916.2014.936996

[11] Hazra, M., Srinivasa, K., and Madhusudhan, G. (2013). Friction welding of a nickel free high nitrogen steel: influence of forge force on microstructure , mechanical properties and pitting corrosion resistance. Integrative Medicine Research, 3(1), 90–100. https://doi.org/10.1016/j.jmrt.2013.12.001

[12] James, J. A., and Sudhish, R. (2016). Study on Effect of Interlayer in Friction Welding for Dissimilar Steels: SS 304 and AISI 1040. Procedia Technology, 25, 1191–1198. https://doi.org/10.1016/j.protcy.2016.08.238

[13] Kalsi, N. S.,and Sharma, V. S. (2011). A statistical analysis of rotary friction welding of steel with varying carbon in workpieces. 957–967. https://doi.org/10.1007/s00170-011- 3361-z

[14] Khany, S. E., Ahmed, S. N. M. G. M. S., Engg, M., College, M. J., and Ap-, H. (2015). An Analytical Study of Dissimilar Materials Joint Using Friction Welding and It ' s Application. 5(2), 1–4.

[15] Kim, S. J., Kong, Y. S., Kim, Y. S., and Kwon, S. W. (2005). On Mechanical Properties of Dissimilar Friction Welded Steel Bars. 300, 2831–2836. https://doi.org/10.4028/www.scientific.net/KEM.297-300.2831

[16] Kohser, R. A., and black, JT (2012). Degarmo's materials and processes in manufacturing. John Wiley and Sons, Inc, Retrieved from http://www.wiley.com/go/returnlabel

[17] Li, P., Li, J., Li, X., Xiong, J., and Zhang, F. (2015). A study of the mechanisms involved in initial friction process of continuous drive friction welding. Journal of Adhesion Science and Technology, 29(12), 1246-1257. https://doi.org/10.1080/01694243.2015.1022499

[18] Li, W., Shi, S., Wang, F., Zhang, Z., and Li, J. (2012). Numerical Simulation of Friction Welding Processes Based on ABAQUS Environment. 5(3), 10–19.

[19] M, M. A., Shrikrishana, K. A., and Sathiya, P. (2015). Finite element modelling and characterization of friction welding on UNS S31803 duplex stainless steel joints. Engineering Science and Technology, an International Journal, 18(4), 704–712. https://doi.org/10.1016/j.jestch.2015.05.002

[20] Mercan, S., Aydin, S., and Özdemir, N. (2015). Effect of welding parameters on the fatigue properties of dissimilar AISI 2205 – AISI 1020 joined by friction welding. International journal of fatigue, 81, 78–90. https://doi.org/10.1016/j.ijfatigue.2015.07.023

[21] Mesmari, H., and Krayem, F. (2013). Mechanical and Microstructure Properties of 304 Stainless Steel Friction Welded Joint. IRJESTI, Int. Research Jrnl. of Eng. Sci., Tech., and Innovation, 2(4), 65–74.

[22] Mohammad, A. K., and Khalil, H. (2016). Effect of Frictional Welding Between Different Stainless-Steel Materials on Their Torsional Properties. 13(6), 113–124. https://doi.org/10.9790/1684-130602113124

[23] Moore,p. (2013). Stainless Steel Grade Datasheets. Atlas steels technical department. Retrieved from www. atlasstels.com.au

[24] Mousavi, A. A. and Kelisham, A. (2016) Experimental Investigation and Statistical Analysis of Friction Welding Parameters for Joining Dissimilar Materials , Al-63400 Alloy and Fe.. 6(6), 21–26.

[25] Nan, X., Xiong, J., Jin, F., Li, X., Liao, Z., and Zhang, F. (2019). Modeling of rotary friction welding process based on maximum entropy production principle. Journal of Manufacturing Processes, 37(1), 21–27. https://doi.org/10.1016/j.jmapro.2018.11.016

[26] Nimesh, P., Chaudhary, R., Singh, R. C., and Ranganath, M. S. (2016). Simulation of Inertia Friction Welding of Mild Steel and Aluminium 6061 using Finite Element Method on ABAQUS .International journal of advanced production and industrial engineering, 1(4), 29-39

[27] Ratkovi, N., Arsi, D., Nikoli, R. R., and Hadzima, B. (2016). Micro-structure in the joint friction plane in friction welding of dissimilar steels. 149, 414–420. https://doi.org/10.1016/j.proeng.2016.06.686

[28] Reddy, A. C. (2015). Fatigue Life Evaluation of Joint Designs for Friction Welding of Mild Steel and Austenite Stainless Steel. 4(2), 1714–1719.

[29] Rombaut, P. (2011). Joining of dissimilar materials through rotary friction welding.

[30] Schmicker, D., Naumenko, K., and Strackeljan, J. (2016). A holistic Approach on the Simulation of Rotary-Friction-Welding. 27(Thaut 2014), 148–150.

[31] Rao, R.V. (2011). Advanced modeling and optimization of manufacturing processes. Springer London Dordrecht Heidelberg New York. https:// doi.org/ 10.1007/978-0- 85729-015-1

[32] Uzkut, M., Ünlü, B. S., and Akdağ, M. (2011). Determination of optimum welding parameters in connecting high alloyed X53CrMnNiN219 and X45CrSi93 steels by friction welding. 34(4), 815–823.

[33] Winiczencko, R. (2015). Effect of friction welding parameters on the tensile strength and microstructural properties of dissimilar AISI 1020-ASTM A536 joints. https://doi.org/10.1007/s00170-015-7751-5

A

APPENDIX

A.1 ***Starting Points***

Number of Starting Points: 112

Tab. A.1: Number of Starting Points: 112

Rotational speed	Friction time	Burn off length
700	4	2
1120	7	3
1120	4	2
900	4	3
700	7	2
1120	10	4
900	7	4
1120	4	4
700	10	3
700	4	4
1120	7	2
900	10	2
728.892	6.40967	3.6679
896.818	7.45315	2.78665
703.263	8.51386	2.12609
1031.94	9.19126	2.31747
759.566	5.17056	2.98685
1064.25	7.60795	3.78297
949.44	4.08684	3.40233
907.78	6.63425	2.78032
1078.03	8.6374	3.00715
725.736	6.21091	2.51492
727.876	9.5638	3.00378
778.203	7.25829	3.5543
1056.69	9.29732	2.4678
909.859	5.10252	2.63264
790.485	8.34587	2.81357
950.046	6.24863	2.01654
1043.61	8.83815	2.94762
862.856	5.41776	3.26889
1014.69	4.71635	3.03319
953.728	6.3678	2.49218
957.919	8.25039	3.75471
770.789	5.2304	3.91624
908.149	7.81142	3.05999
1074.41	8.91096	2.05046
943.011	9.89535	2.45123
911.548	9.2937	3.16566
805.932	7.41843	3.88231
1103.13	4.99986	3.80265
820.282	9.46449	3.90503
709.677	7.58992	3.75995

760.087	4.42006	3.50223
1113.69	7.19296	2.86349
722.813	7.37562	3.22276
778.092	5.66736	3.43312
796.675	8.31628	3.67246
968.951	5.35653	2.56209
1000.89	8.01009	2.19141
1112.12	6.59434	3.85287
996.114	9.84251	2.42318
730.491	6.69229	3.06982
871.922	5.55624	2.05657
1020.28	4.38558	2.71289
908.929	5.75661	2.04628
886.189	4.83117	3.04542
1051.76	8.41554	3.71027
1099.25	9.60344	3.67156
828.303	7.68749	2.15126
1114.82	9.40413	2.45169
951.412	4.61528	2.18256
917.073	8.8058	2.37114
827.258	8.31584	2.66725
818.204	9.61547	3.55248
858.717	8.22353	2.34873
789.675	6.22584	2.89285
922.103	6.92404	3.17635
1090.38	8.89297	2.5778
874.587	4.17482	2.35335
942.694	6.37145	2.61647
1003.1	4.33344	3.13002
1037.1	4.5451	2.17567
1052.7	8.76373	2.33532
1088.76	6.6319	3.73393
747.102	9.36854	2.90049
1102.67	9.47874	3.96992
752.806	8.30465	2.9336
799.947	8.14952	2.44009
1031.49	6.18015	2.65533
760.101	7.44103	3.61423
742.304	9.32392	2.60289
827.393	7.76834	3.03242
936.843	9.11856	2.93833
748.621	8.01149	2.29047
709.859	8.69668	3.21358

771.1	4.76396	2.93353
957.682	8.9017	2.56291
909.917	5.337	2.70633
1076.12	7.52158	3.01108
834.066	5.00963	2.13717
987.844	5.28631	2.84447
1075.11	9.84967	2.91319
1069.52	4.43627	2.18133
898.124	8.96947	3.61473
1026.77	7.60194	2.5803
862.139	7.89212	2.21488
775.911	6.20302	3.90976
716.028	9.21103	2.79805
1033.61	4.61152	3.1517
852.383	5.73399	2.85934
732.744	9.55923	3.75334
777.514	7.65212	3.57042
1044.48	9.23074	3.17298
1029.31	7.45166	3.58902
715.145	9.85078	2.32391
781.143	9.65935	2.82472
762.829	9.98455	2.52014
932.804	8.66553	2.99031
920.306	9.50595	3.83266
842.99	4.65468	2.71646
1071.54	4.8063	3.07519

A.2 ***Solutions***

Tab. A.2: 42 Solutions found

Number	Rotational speed	Friction time	Burn off length	UTS	StdErr(UTS)	Desirability
1	1101.195	7.987	3.734	553.762	6.292	0.994 Selected
2	1101.143	8.011	3.733	553.761	6.292	0.994
3	1100.901	7.970	3.729	553.757	6.292	0.994
4	1101.654	7.993	3.743	553.751	6.292	0.994
5	1100.571	7.995	3.723	553.748	6.292	0.994
6	1100.768	7.944	3.728	553.743	6.292	0.994
7	1101.578	8.044	3.741	553.741	6.292	0.994
8	1101.809	8.024	3.745	553.741	6.292	0.994
9	1101.792	7.963	3.747	553.728	6.292	0.994
10	1102.441	8.049	3.759	553.665	6.292	0.994
11	1102.389	7.952	3.761	553.638	6.292	0.994
12	1102.602	8.094	3.763	553.600	6.292	0.994
13	1098.789	7.937	3.697	553.582	6.292	0.994
14	1100.574	8.151	3.723	553.572	6.292	0.994
15	1101.248	8.163	3.735	553.571	6.292	0.994
16	1097.096	7.941	3.674	553.320	6.292	0.993
17	1101.877	7.586	3.802	551.927	6.292	0.992
18	1099.814	7.324	3.776	550.916	6.292	0.991
19	1099.693	8.236	3.923	547.797	6.292	0.988
20	1086.612	6.909	3.590	547.624	6.292	0.988
21	1094.099	6.733	3.682	547.561	6.292	0.988
22	1120.000	5.627	2.495	546.768	6.292	0.987
23	1119.981	5.598	2.504	546.756	6.292	0.987
24	1119.934	5.649	2.490	546.759	6.292	0.987
25	1119.589	5.613	2.505	546.742	6.292	0.987
26	1119.328	5.639	2.501	546.728	6.292	0.987
27	1119.230	5.699	2.484	546.681	6.292	0.987
28	1118.595	5.647	2.508	546.676	6.292	0.987
29	1118.449	5.663	2.505	546.662	6.292	0.987
30	1118.218	5.604	2.525	546.621	6.292	0.987
31	1117.121	5.671	2.520	546.541	6.292	0.987
32	1119.995	5.424	2.549	546.370	6.292	0.986
33	1115.729	5.590	2.560	546.293	6.292	0.986
34	1119.871	5.840	2.430	546.245	6.292	0.986
35	1115.216	5.791	2.507	546.236	6.292	0.986
36	1115.107	5.857	2.487	546.068	6.292	0.986
37	1119.999	5.861	2.419	546.047	6.288	0.986
38	1119.998	5.909	2.404	545.802	6.292	0.986
39	1119.980	4.891	2.631	541.642	6.291	0.981
40	1085.225	5.836	3.432	539.985	6.292	0.980
41	1078.140	9.152	3.760	538.777	6.292	0.979
42	1085.282	5.324	3.171	535.919	6.292	0.976

A.3 ***Spectrometer results***

Fig. A.1: Spectrometer results